



OPEN ACCESS

EDITED BY

Thales Renato Ochotorena De Freitas,
Federal University of Rio Grande do
Sul, Brazil

REVIEWED BY

Erik Seiffert,
University of Southern California,
United States
Daniela C. Kalthoff,
Swedish Museum of Natural History,
Sweden

*CORRESPONDENCE

Germán Montoya-Sanhueza
g.montoya.sanhueza@gmail.com

SPECIALTY SECTION

This article was submitted to
Behavioral and Evolutionary Ecology,
a section of the journal
Frontiers in Ecology and Evolution

RECEIVED 18 January 2022

ACCEPTED 06 June 2022

PUBLISHED 20 October 2022

CITATION

Montoya-Sanhueza G, Bennett NC,
Chinsamy A and Šumbera R (2022)
Functional anatomy and disparity
of the postcranial skeleton of African
mole-rats (Bathyergidae).
Front. Ecol. Evol. 10:857474.
doi: 10.3389/fevo.2022.857474

COPYRIGHT

© 2022 Montoya-Sanhueza, Bennett,
Chinsamy and Šumbera. This is an
open-access article distributed under
the terms of the [Creative Commons
Attribution License \(CC BY\)](https://creativecommons.org/licenses/by/4.0/). The use,
distribution or reproduction in other
forums is permitted, provided the
original author(s) and the copyright
owner(s) are credited and that the
original publication in this journal is
cited, in accordance with accepted
academic practice. No use, distribution
or reproduction is permitted which
does not comply with these terms.

Functional anatomy and disparity of the postcranial skeleton of African mole-rats (Bathyergidae)

Germán Montoya-Sanhueza^{1,2*}, Nigel C. Bennett³,
Anusuya Chinsamy² and Radim Šumbera¹

¹Department of Zoology, Faculty of Science, University of South Bohemia, České Budějovice, Czechia, ²Department of Biological Sciences, University of Cape Town, Cape Town, South Africa, ³Department of Zoology and Entomology, Mammal Research Institute, University of Pretoria, Pretoria, South Africa

The burrowing adaptations of the appendicular system of African mole-rats (Bathyergidae) have been comparatively less investigated than their cranial adaptations. Because bathyergids exhibit different digging modes (scratch-digging and chisel-tooth digging) and social systems (from solitary to highly social), they are a unique group to assess the effects of distinct biomechanical regimes and social organization on morphology. We investigated the morphological diversity and intraspecific variation of the appendicular system of a large dataset of mole-rats ($n = 244$) including seven species and all six bathyergid genera. Seventeen morpho-functional indices from stylopodial (femur, humerus) and zeugopodial (ulna, tibia-fibula) elements were analyzed with multivariate analysis. We hypothesized that scratch-diggers (i.e., *Bathyergus*) would exhibit a more specialized skeletal phenotype favoring powerful forelimb digging as compared to the chisel-tooth diggers, and that among chisel-tooth diggers, the social taxa will exhibit decreased limb bone specializations as compared to solitary taxa due to colony members sharing the costs of digging. Our results show that most bathyergids have highly specialized fossorial traits, although such specializations were not more developed in *Bathyergus* (or solitary species), as predicted. Most chisel tooth-diggers are equally, or more specialized than scratch-diggers. *Heterocephalus glaber* contrasted significantly from other bathyergids, presenting a surprisingly less specialized fossorial morphology. Our data suggests that despite our expectations, chisel-tooth diggers have a suite of appendicular adaptations that have allowed them to maximize different aspects of burrowing, including shoulder and neck support for forward force production, transport and removal of soils out of the burrow, and bidirectional

locomotion. It is probably that both postcranial and cranial adaptations in bathyergids have played an important role in the successful colonization of a wide range of habitats and soil conditions within their present distribution.

KEYWORDS

fossorial adaptation, bone morphology, scratch-digging, chisel-tooth digging, sociality, evolution, *Heterocephalus glaber*

“Africa has produced many mammal curiosities, and the Bathyergidae take a high rank among these”

JR Ellerman, 1956

Introduction

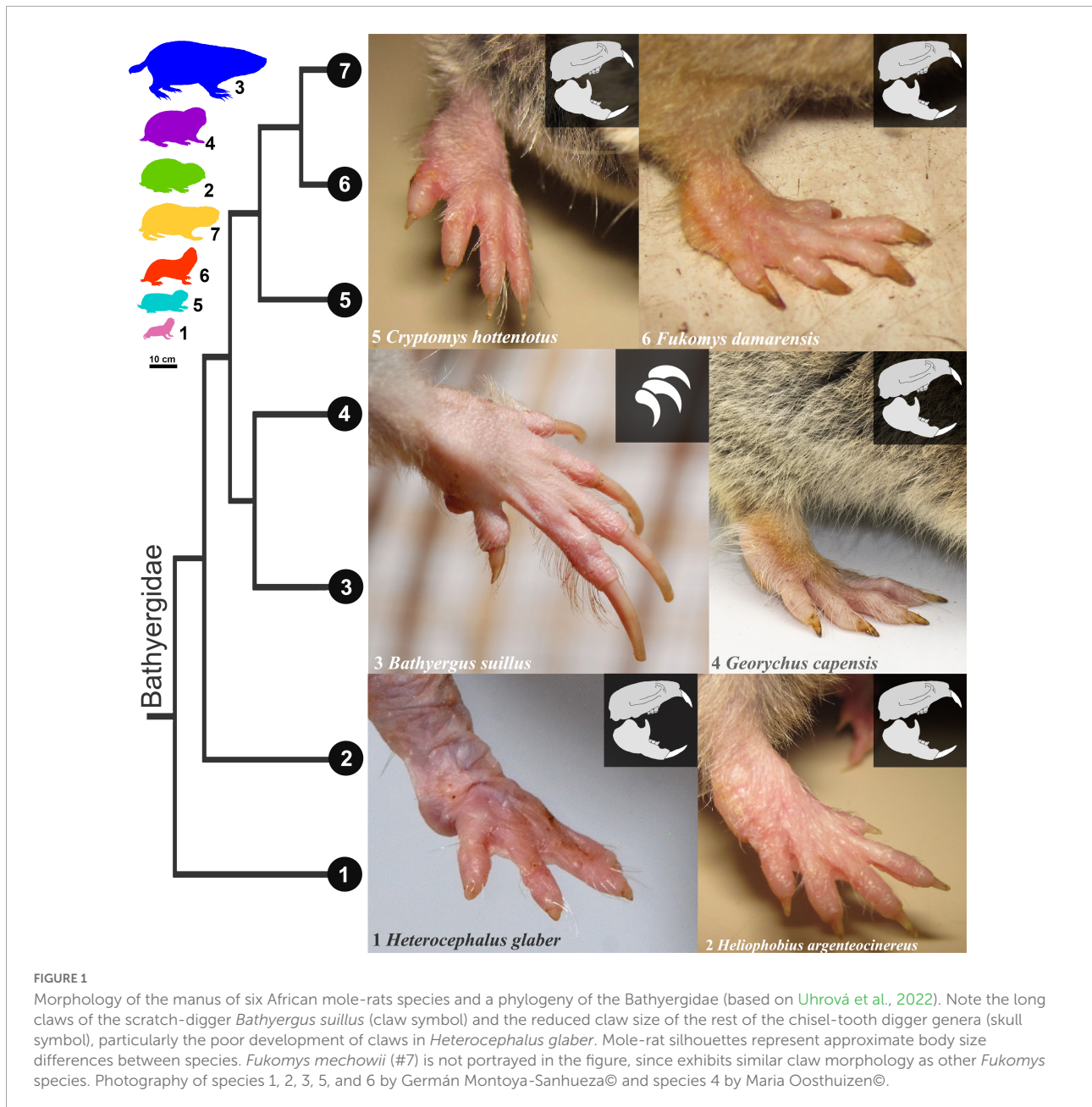
African mole-rats (Bathyergidae) are highly specialized subterranean rodents that spend most of their lives underground and build extensive and complex burrow systems (Jarvis et al., 1998; Bennett and Faulkes, 2000; Le Comber et al., 2002). Among bathyergids, only one genus (*Bathyergus*) is a scratch-digger that predominantly uses its long fore-claws to break up mostly sandy soils, while the rest of the bathyergids (*Heliophobius*, *Georychus*, *Cryptomys*, *Fukomys*, and *Heterocephalus*) are chisel-tooth diggers that primarily use their highly procumbent incisors to break up soils of different degrees of hardness, varying from sandy to highly compacted (Jarvis and Sale, 1971; Bennett and Faulkes, 2000). Additionally, all the chisel tooth-digging genera have very short claws in the forefeet and hindfeet (Figure 1), thus suggesting a more relegated function of claws for breaking up soils. Bathyergids also have a wide spectrum of social organizations ranging from solitary to highly social (Jarvis and Bennett, 1993; Jarvis et al., 1994; Burda et al., 2002), as well as a wide range of body sizes, from ~35 g in *Heterocephalus glaber* up to 2 kg in *Bathyergus suillus*. Such combination of features makes African mole-rats a unique group of mammals to assess the effects of digging mode and social behavior on the morphology of the burrowing apparatus.

Although many aspects of their ecology, physiology, behavior, and evolutionary history have been well-documented (e.g., Bennett and Faulkes, 2000; Šumbera, 2019; Visser et al., 2019; Oosthuizen and Bennett, 2022), a comparative assessment of their postcranial morphology and development including all genera is still lacking. The fossil record of this group is underrepresented, and most fossil taxa are known basically on their cranial and dental material only (Lavocat, 1973; Winkler et al., 2010; Bento Da Costa and Senut, 2022). Several studies of extant bathyergids have focused on the cranial and dental anatomy of a few species (e.g., Berkovitz and Faulkes, 2001;

Hart et al., 2007; Barčiová et al., 2009; Van Daele et al., 2009; Gomes Rodrigues et al., 2011; McIntosh and Cox, 2016a; Caspar et al., 2021). Only more recent assessments have incorporated a comparative approach including a larger number of species (Gomes Rodrigues and Šumbera, 2015; Gomes Rodrigues et al., 2016; Mason et al., 2016; McIntosh and Cox, 2016b; Fournier et al., 2021). In general, these studies have found clear differences between chisel-tooth diggers and scratch-diggers, with the former having a more specialized dental and craniomandibular morphology, including more procumbent incisors, shorter snout, relatively wider and taller skulls with enlarged zygomatic arches, strongly hystricognathous mandible, and increased jaw and condyle lengths relative to their size, all features that facilitates higher bite forces and wider gapes to maximize breaking up soils (Gomes Rodrigues et al., 2016; McIntosh and Cox, 2016a,b).

Regarding their limb anatomy, several studies on rodents and mammals have included a few bathyergid species in their analyses, although these are usually represented by small sample sizes or are still unpublished (e.g., Carleton, 1941; Cuthbert, 1975; Hildebrand, 1978, 1985; De Graaff, 1979; Stein, 2000; Samuels and Van Valkenburgh, 2008; Thomas, 2013; Prochel et al., 2014; Wilson and Geiger, 2015). Recently, Sahd et al. (2019) assessed the effects of hind-foot drumming in the musculoskeletal system of *B. suillus*, *Georychus capensis*, and *Cryptomys hottentotus natalensis*, and Doubell et al. (2020) compared the forelimb musculoskeletal anatomy of *B. suillus* and *H. glaber*. Also, Montoya-Sanhueza and Chinsamy (2018) and Montoya-Sanhueza et al. (2019) focused on the postnatal development of the long bones and the patterns of mineral mobilization (bone formation and resorption) of the femur of *B. suillus*, respectively. More recently, Montoya-Sanhueza et al. (2022a,b) assessed the development of bone superstructures associated with fossoriality, and the proximal morphology of the femur of a large sample including all bathyergid genera. The latter studies represent the first comparative assessments of the limb anatomy including all bathyergid genera.

The present study aims to determine the patterns of intraspecific and interspecific variation of the appendicular digging apparatus of Bathyergidae. We quantified the morphological diversity (disparity) of the humerus, ulna, femur and tibia-fibula of all six bathyergid genera including



seven species (Table 1). We assessed the relationship between morphology and behavior (i.e., digging mode and social organization) in this family, and predicted that the scratch-digging taxa (i.e., *Bathyergus*) would exhibit a more specialized skeletal phenotype favoring powerful parasagittal motion of forearms and downward thrust of the forefeet to break up the soil as compared to the chisel-tooth digging taxa, because their limbs are directly involved in breaking the soils during the initial phase of burrowing. Thus, *Bathyergus* should exhibit a more distally located deltoid tuberosity to increase the lever arm for powerful retraction and flexion of the humerus, as well as an enlarged olecranon process to increase the power

stroke of the arm during elbow extension (Vassallo, 1998). Because the hindlimb skeleton is assumed to perform relatively similar functions in both scratch-diggers and chisel-tooth diggers, involving body stabilization and soil transport/removal (Gambaryan and Gasc, 1993; Stein, 2000; Moore Crisp et al., 2019), we expect similar levels of specialization among species.

We also examined if social organization has an effect on morphological variation. It is known that *H. glaber* forms organized sequences of “cooperative” digging, where colony members work together in a relay forming chains (Jarvis and Sale, 1971; Tucker, 1981), although this behavior is probably also present in other social bathyergids (Šumbera., 2019). It

TABLE 1 Main characteristics of the seven bathyergid species analyzed in this study.

| Common name | Species | Sample size | Digging mode | Social system |
|---------------------|--------------------------------------|-------------|----------------------|---------------|
| Naked mole-rat | <i>Heterocephalus glaber</i> | 65 | Chisel-tooth digging | Highly social |
| Silvery mole-rat | <i>Heliophobius argenteocinereus</i> | 29 | Chisel-tooth digging | Solitary |
| Cape dune mole-rat | <i>Bathyergus suillus</i> | 39 | Scratch-digging | Solitary |
| Cape mole-rat | <i>Georchus capensis</i> | 33 | Chisel-tooth digging | Solitary |
| Common mole-rat | <i>Cryptomys hottentotus</i> | 34 | Chisel-tooth digging | Social |
| Giant mole-rat | <i>Fukomys mechowii</i> | 12 | Chisel-tooth digging | Highly social |
| Damaraland mole-rat | <i>Fukomys damarensis</i> | 32 | Chisel-tooth digging | Highly social |

has been documented that increased group size in mole-rats lowers the costs of foraging in the social *C. hottentotus* (Spinks and Plagányi, 1999), that solitary species such as *Heliophobius argenteocinereus* have a more effective working metabolism as compared to *Fukomys mechowii* (Zelová et al., 2010), and that the increased number of non-breeding subordinates in *Fukomys damarensis* is associated with reductions in the workload of breeders (Housley et al., 2020). These data suggest that social species may share the effort of digging activities, probably reducing the selection of an extremely specialized burrowing apparatus. Consequently, we also expect solitary species to exhibit increased mechanical advantage in their limb bones as compared to social species.

Materials and methods

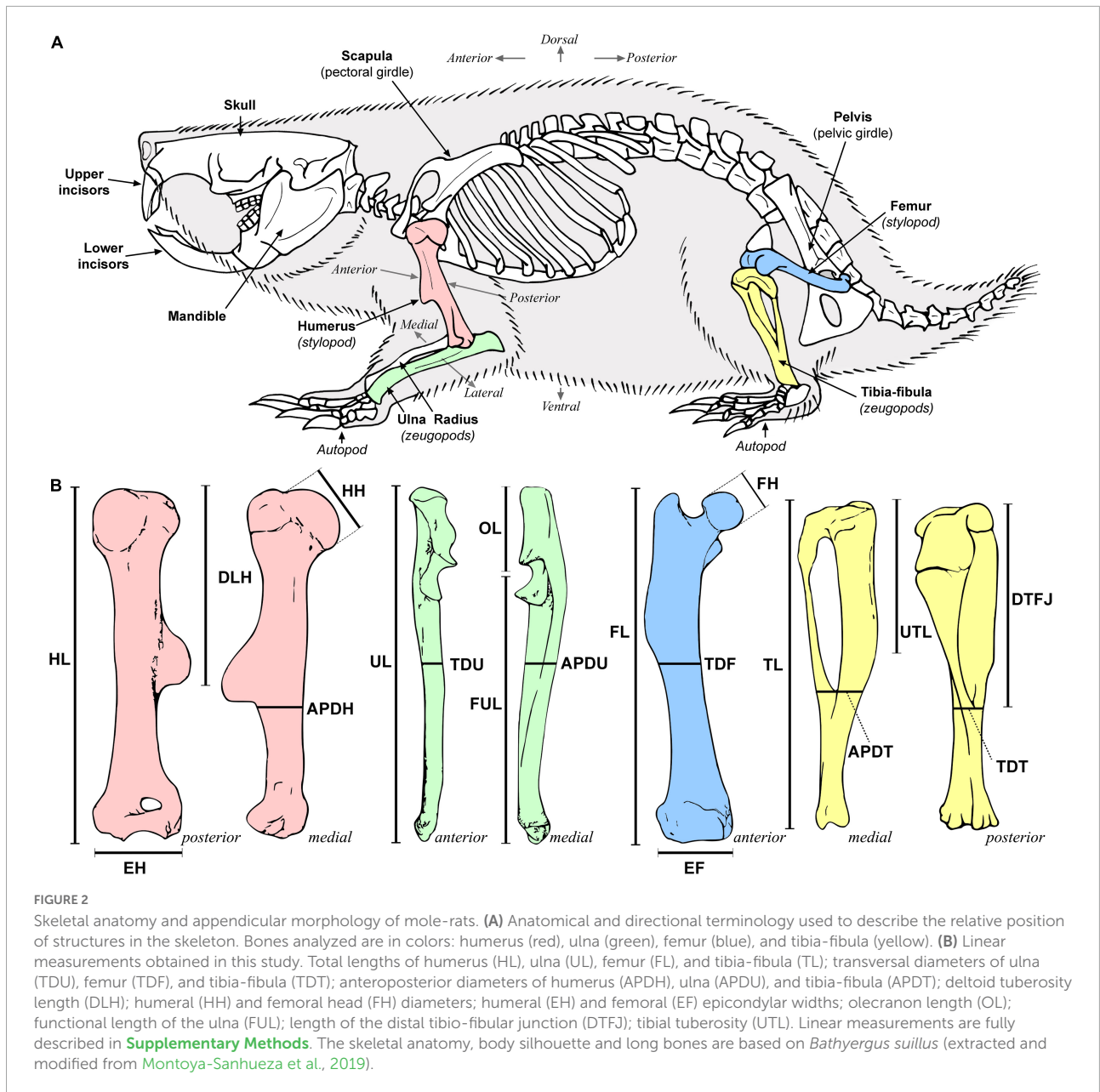
Specimens and skeletal maturity

A total of 244 specimens comprising seven species of all six bathyergid genera were analyzed (Table 1 and Figure 1). The sample comprises skeletally mature specimens of both sexes, as well as individuals of unknown sex. Body mass (BM) was obtained for almost all individuals. In this study, skeletal maturity is defined as individuals having full alveolar eruption of all upper or lower molars. Patterns of molar eruption were obtained using dental information from multiple sources (Hamilton, 1928; Taylor et al., 1985; Bennett et al., 1990; Jarvis and Sherman, 2002; Hart et al., 2007; Gomes Rodrigues et al., 2011; Gomes Rodrigues and Šumbera, 2015; Berkovitz and Shellis, 2018; Montoya-Sanhueza et al., 2021a,b). The skeletal maturity of specimens lacking craniodental material was based on gross morphological features of the body and limbs, such as having an adult body size and/or well-developed limbs showing fully developed secondary centers of ossification at epiphyses and a fused distal epiphysis of the humerus (e.g., Klein, 1991). The majority of the specimens were wild-caught, although some individuals of *F. damarensis* and *F. mechowii*, and all individuals of *H. glaber* were born in captivity. The colonies of *H. glaber* were housed in tunnels made of glass without substrate to dig in. Additional details of captivity conditions for *H. glaber*

are described elsewhere (Montoya-Sanhueza et al., 2021a). All material analyzed here is housed in the Department of Biological Sciences at the University of Cape Town (UCT), South Africa.

Functional anatomy and morpho-functional indices

Stylopodial (femur and humerus) and zeugopodial (ulna and tibia-fibula) elements from either the right or left side of the individual were dissected and skeletonized. The general anatomy of each bone was described and compared among species following the anatomical nomenclature of previous studies (e.g., Holliger, 1916; Greene, 1935; Salton and Sargis, 2008, 2009; Böhmer et al., 2020; Figure 2A). A detailed description of the main anatomical characteristics of the long bones of bathyergids is presented in the Supplementary Figures 1, 2. A total of 19 linear measurements including length and diameter of limb bones were obtained (Figure 2B), mostly based on Echeverría et al. (2014) and Montoya-Sanhueza et al. (2019), and the references therein. All measurements were recorded to the nearest 0.01 mm using a digital caliper, and are fully described in Supplementary material. Seventeen morpho-functional indices (Table 2) that reflect the main aspects of the bone shape at the diaphyseal, proximal and distal portions of the bone were calculated from linear measurements following previous studies (Howell, 1965; Hildebrand, 1985; Rose, 1989; Vizcaíno et al., 1999, 2016; Elissamburu and Vizcaíno, 2004; Salton and Sargis, 2008; Samuels and Van Valkenburgh, 2008; Echeverría et al., 2014; Wilson and Geiger, 2015; Montoya-Sanhueza et al., 2019; and references therein). These morpho-functional indices represent an easy and straightforward approximation to estimate mechanical advantage and function of the main muscles related to limb function, specifically for scratch-digging (e.g., Hildebrand, 1985; Samuels and Van Valkenburgh, 2008). In particular, we follow the study of Montoya-Sanhueza et al. (2019), which reviewed and modified some previous functional indices to appropriately assess the functional implications of parasagittal scratch-digging with the forelimb and strength of the hindlimb. In total, four indices represent the morphology of the humerus (RDT, HRI,



EIH, HH), four of the ulna (IFA, URI, URI*, BI), three of the femur (FRI, EIF, FHI) and five of the tibia-fibula (TSI, TRI, TRI*, TJI, CI) (Table 2). The BI, CI and an additional index, the intermembral index (IMI) represent proportions between bone elements, thus indicating locomotor advantage (Howell, 1965). Since *H. glaber* lacks some relevant bone superstructures in their long bones (i.e., lack of a projected deltoid tuberosity and non-fused tibia and fibula, Montoya-Sanhueza et al., 2022a), the indices RDT, TRI, TRI* and TJI were not calculated for this taxon. The calculation and functional significance of all indices are presented in Table 2. Additionally, because sex differences are known to affect the growth trajectories and morphology of small mammals, sexual

dimorphism in body mass and morpho-functional indices was also assessed.

Ecomorphological groups

To assess the effects of a specific subterranean lifestyle on bone phenotype, three ecomorphological groups that account for the main behavioral and functional features of bathyergids were established based on a combination of their digging mode and social organization, and are classified as follow: (i) solitary scratch-diggers, (ii) solitary chisel-tooth diggers, and (iii) social chisel-tooth diggers. Note that the hypothetical group of “social

scratch-diggers” was not defined in the present study since there are no extant bathyergid species reported with such combination of features.

Statistical analysis

Multivariate analysis

A series of multivariate analysis of variance (MANOVA) coupled with Tamhane *post hoc* tests were carried out to assess interspecific differences in morpho-functional indices. Forelimb ($n = 244$) and hindlimb ($n = 217$) data sets were not equal in completeness, so these were assessed separately. This allowed emphasizing differences between limb regions. Because some morpho-functional indices were not calculated for *H. glaber* (see above), two MANOVAs were performed for each limb region, one including all species but excluding some indices, and a second including all indices, but excluding *H. glaber*. This allowed the testing of differences in bone morphology and fossorial specializations with and without the influence of *H. glaber*. Homoscedasticity of the sample was tested by \log_{10} transformation, although without improvement, so the data were analyzed without transformation. Consequently, because all MANOVAs showed unequal variances, both Wilks' lambda and Pillai trace statistics are provided, since the latter test is more robust under violations of homoscedastic covariance (Quinn and Keough, 2002). Graphs (bar charts) were prepared for all indices and show mean (central point), standard error (s.e., shorter whiskers) and standard deviation (s.d., longer whiskers). Morphological data are presented as mean and standard deviation (mean \pm s.d.). A significance level of 0.05 was used for all analyses.

Ordination analysis

Principal Component Analysis (PCA) and Discriminant Analysis (LDA) were performed to identify the major components of variation among the seven species and the three ecomorphological groups, respectively. The PCA used separated datasets for forelimbs ($n = 244$) and hindlimbs ($n = 217$), and specimens with an incomplete dataset of indices (either for the forelimb and hindlimb) were still included, but performing the “iterative imputation” method as an estimation for the missing values. For the LDA, forelimb and hindlimb indices were combined, and only specimens ($n = 216$) with a complete set of measurements (i.e., for humerus, ulna, femur, and tibia-fibula) were analyzed. The LDA produces linear combinations of variables (canonical variates) that best separate *a priori* defined groups, based on maximizing differences between groups and reducing their within-group differences. MANOVAs were coupled to the LDA to assess

differences among ecomorphological groups. We also estimated whether specimens could be classified into a defined group. As in the multivariate analysis, separated PCAs and DAs were performed (see above), a dataset including all species, and a dataset including all indices. All datasets included individuals of known and unknown sex. The algorithm to assess the correlation matrix for the PCA was the “variance-covariance,” since all the linear measurements used to build the indices were originally measured in the same unit (mm). Variables were analyzed to highlight “between group” (species and ecomorphological) differences.

Sex differences

Sex differences in both body mass (BM) and morpho-functional indices were assessed by non-parametric two-tailed (Wilcoxon) Mann-Whitney *U*-test, and two-way PERMANOVA for all species ($n = 190$) and indices, coupled with Bonferroni correction (excluding *H. glaber*), respectively. One-way PERMANOVA was used to test sex differences in *H. glaber* ($n = 59$). A significance level of 0.05 was used for all analyses, and *p*-values were obtained using 9,999 permutations. In total, 139 females and 110 males were analyzed.

All analyses and plots were performed in PAST version 2.17c (Hammer et al., 2001) and IBM SPSS version 25 (IBM Corp, 2017).

Results

A qualitative description of the forelimb and hindlimb anatomy of bathyergids is presented in the [Supplementary Results](#). Also refer to Montoya-Sanhueza et al. (2022a,b).

Multivariate analysis of the forelimb

The main characteristics of the forelimb are presented in [Figure 3A](#). Descriptive statistics of the morpho-functional indices are presented in [Table 3](#), and corresponding whisker plots in [Figure 3B](#). The MANOVA including all species (and excluding RDT) showed significant differences among species [Wilks' $\lambda = 0.013$; $F_{(42,1086)} = 38.961$; $p < 0.001$] ([Table 4](#)). The variables that better explain morphological differences can be identified by high “partial eta squared” (PES) values (> 0.50), which accounts for the proportion of variance explaining interspecific differences. All indices, except URI showed high PES values, ranging between 0.504 (IFA) and 0.697 (BI) ([Table 4](#) and [Supplementary Table 1](#)). In the humerus, HRI showed the highest PES values (0.566), thus contributing most to species differentiation, while BI (0.697) and URI* (0.590) showed the highest PES in the ulna. In this analysis, *H. glaber*

TABLE 2 Morpho-functional indices, calculation, and functional significance.

| Index | | Calculation | Functional significance |
|-------|---|---|--|
| RDT | Relative position of the deltoid tuberosity | Humeral head-distal origin of deltoid process length divided by humeral length (DLH/HL) | An estimator of in-lever arm of the deltoid and pectoral muscles. Higher values (more distally located DT) indicate stronger flexion of the arm. |
| HRI | Humerus robustness index | Anteroposterior diameter at diaphysis divided by humeral length (APDH/HL) | Indicates robustness of the humerus and its ability to resist bending and torsional stresses, mainly in the anteroposterior axis. |
| EIH | Humeral epicondylar index | Epicondylar width of the humerus divided by humeral length (EH/HL) | Indicates the relative area available for the origin of the forearm flexors, pronators, and supinators. |
| HHI | Humeral head index | Maximum diameter (anteroposterior) of humeral head divided by humeral length (HH/HL) | Represents the relative size of the articular surface of the glenohumeral joint, and gives an idea of the area available for stabilization and shock absorption of the shoulder needed for digging, as well as extensiveness for anteroposterior movements of the humerus. |
| IFA | Index of fossorial ability | Olecranon length divided by the functional ulnar length (OL/FUL) | This index reflects the mechanical advantage of the triceps and epitrochlearis muscles during elbow extension. |
| URI | Robustness of the ulna (ML) | Mediolateral (transverse) diameter of the ulna at the diaphyseal midpoint divided by functional ulnar length (TDU/FUL) | Reflects the resistance of the ulna to bending in the mediolateral axis. |
| URI* | Robustness of the ulna (AP) | Anteroposterior diameter of the ulna at the diaphyseal midpoint divided by functional ulnar length (APDU/FUL) | Reflects the resistance of the ulna to bending in the anteroposterior axis, as well as indicates the relative surface available for the insertion of muscles involved in pronation and supination of the forearm, and flexion of the manus and digits. |
| BI | Brachial index | Functional ulnar length divided by humeral length (FUL/HL) | Indicates the relative proportions of proximal (humerus) and middle (ulna) elements of the forearm, and gives an indication of the extent to which the forelimb is apt for fast movements. |
| FRI | Femur robustness index | Transverse diameter of the femur at the diaphyseal midpoint divided by the functional femoral length (TDF/FL) | Indicates robustness of the femur and its ability to resist bending and torsional stresses in the mediolateral axis. |
| EIF | Femoral epicondylar index | Epicondylar width of the femur divided by femoral length (EF/FL) | Indicates the relative area available for the origin of the gastrocnemius, extensor and flexor muscles used mainly for flexion of the knee and plantar-flexion of the pes. |
| FHI | Femoral head index | Maximum diameter of femoral head divided by femoral length (FH/FL) | Indicates the dimension of the femoral head, and gives an idea of the range of motion of the hip joint. |
| TSI | Tibial crest index | Proximal tibia length (distance from the proximal articular surface of the tibia to the distal point of the tibial tuberosity), divided by the tibial length (UTL/TL) | Reflects the strength of the leg and the relative width available for the insertion of the gracilis, semitendinosus and semimembranosus muscles and the foot flexors. Also hamstrings and biceps femoris muscles acting across the knee and hip joints. |
| TRI | Robustness of the tibia-fibula (ML) | Mediolateral (transverse) diameter of the tibia-fibula divided by the tibial length (TDT/TL) | Indicates robustness of the tibia and its ability to resist bending and torsional stresses in the mediolateral axis. |
| TRI* | Robustness of the tibia-fibula (AP) | Anteroposterior diameter of the tibia-fibula divided by the tibial length (APDT/TL) | Indicates robustness of the tibia and its ability to resist bending and torsional stresses in the anteroposterior axis. |
| TJI | Tibio-fibular junction index | Length of the distal tibio-fibular junction divided by the tibial length (DTFJ/TL) | Indicates the extension of the tibio-fibular fusion along the distal diaphysis, and hence the resistance to bending and torsional loads during biomechanically demanding activities against the substrate. Lower values indicate a larger fusion area, and therefore a stronger diaphysis. |
| CI | Crural index | Tibial length divided by femoral length (TL/FL) | Indicates the relative proportions of proximal (femur) and middle (tibia) elements of the hindleg. Indicates how well the hindlimbs are apt for speed. |
| IMI | Intermembral index | Forelimb length divided by the hindlimb length [(HL + FUL)/(FL + TL)] | Indicates the relative symmetry between the foreleg and hindleg. |

Measurements are illustrated in [Figure 2](#), and described in [Supplementary Methods](#). Indices are based on [Echeverría et al. \(2014\)](#) and [Montoya-Sanhueza et al. \(2019\)](#), and references therein. Anteroposterior (AP), mediolateral (ML).

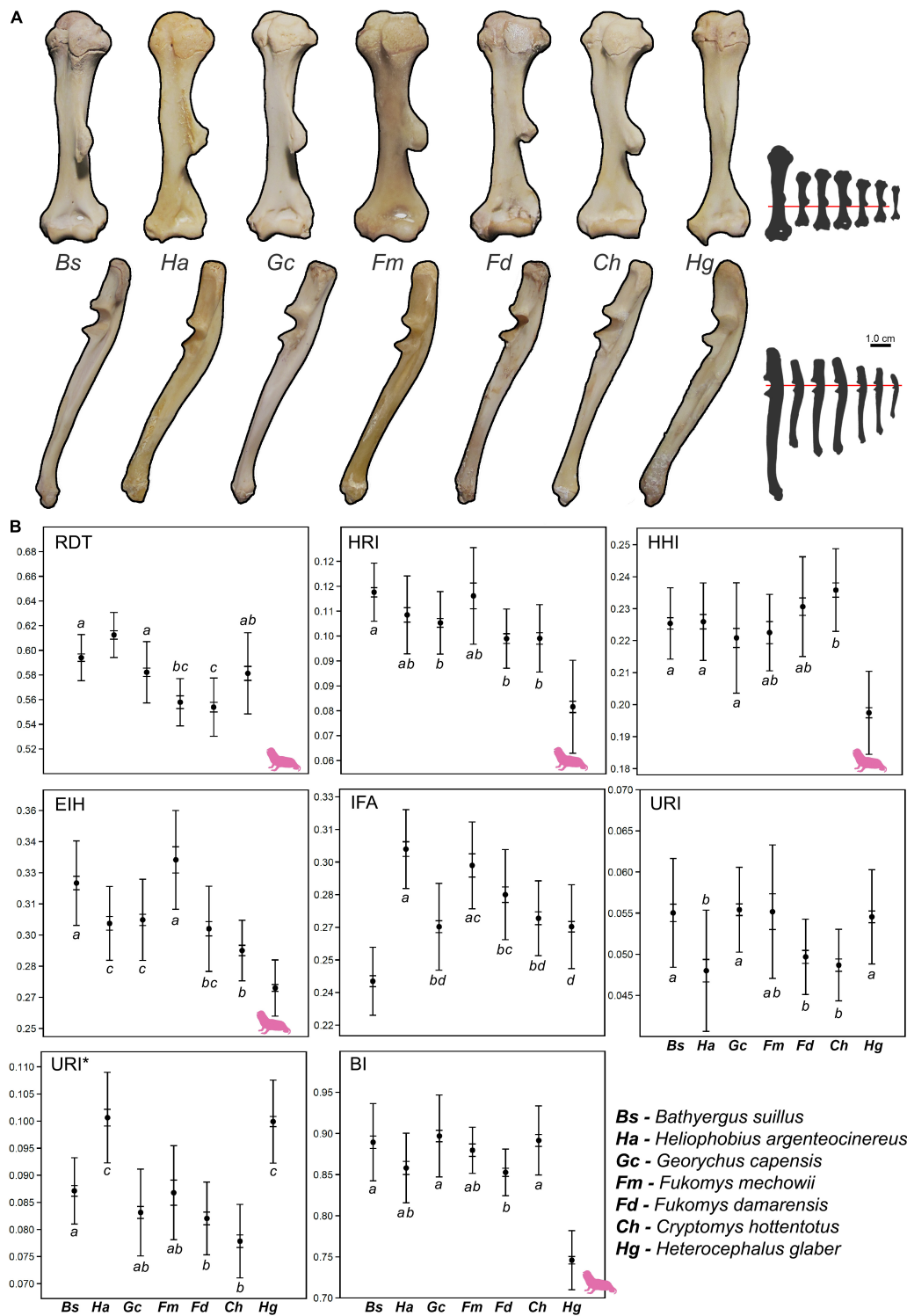


FIGURE 3

Quantification of the forelimb morphology (humerus and ulna). (A) Humeral (top row) and ulnar (bottom row) morphology of all species. Bones scaled to same size to emphasize differences in bone shape. Small bone silhouettes show the real relative size of bones between species. The humeri are aligned to the distal origin of the deltoid tuberosity (except in *Heterocephalus glaber*), while the ulnae are aligned to the center of the trochlear notch. (B) Whisker plots showing differences among species. Mean (central point), s.e (short whiskers) and s.d. (long whiskers). Species that share the same letter represent homogeneous subsets, as identified by *post hoc* (Tamhane) tests. The pink silhouette represents *H. glaber* and indicates the indices for which this species differs significantly from other bathyergids, as well as the indices not measured for this species (i.e. lack of morphological specialization). Taxa are primarily ordered from solitary to social species, and secondarily from the largest to the smallest species. Abbreviation of indices in Table 2.

TABLE 3 Descriptive statistics (mean and s.d.) of forelimb and hindlimb morpho-functional indices.

| Index | <i>B. suillus</i> | <i>He. argenteoci nereus</i> | <i>G. capensis</i> | <i>F. mechowii</i> | <i>F. damarensis</i> | <i>C. hottentotus</i> | <i>H. glaber</i> | Bathyergidae** | Bathyergidae |
|----------|-------------------|------------------------------|--------------------|--------------------|----------------------|-----------------------|------------------|----------------|--------------|
| Forelimb | (n = 39) | (n = 29) | (n = 33) | (n = 12) | (n = 32) | (n = 34) | (n = 65) | (n = 179) | (n = 244) |
| RDT | 0.594 | 0.612 | 0.587 | 0.559 | 0.554 | 0.581 | – | 0.581 | – |
| s.d. | 0.019 | 0.018 | 0.020 | 0.017 | 0.024 | 0.033 | – | 0.022 | – |
| HRI | 0.118 | 0.111 | 0.111 | 0.114 | 0.105 | 0.104 | 0.084 | 0.111 | 0.107 |
| s.d. | 0.009 | 0.012 | 0.009 | 0.013 | 0.009 | 0.010 | 0.014 | 0.005 | 0.011 |
| HHI | 0.225 | 0.226 | 0.220 | 0.223 | 0.231 | 0.236 | 0.197 | 0.227 | 0.223 |
| s.d. | 0.011 | 0.012 | 0.017 | 0.012 | 0.015 | 0.013 | 0.013 | 0.006 | 0.012 |
| EIH | 0.325 | 0.306 | 0.308 | 0.329 | 0.302 | 0.293 | 0.274 | 0.310 | 0.305 |
| s.d. | 0.020 | 0.018 | 0.020 | 0.016 | 0.021 | 0.015 | 0.014 | 0.014 | 0.019 |
| IFA | 0.245 | 0.306 | 0.276 | 0.303 | 0.288 | 0.274 | 0.270 | 0.282 | 0.280 |
| s.d. | 0.016 | 0.018 | 0.019 | 0.018 | 0.018 | 0.017 | 0.019 | 0.022 | 0.021 |
| URI | 0.055 | 0.048 | 0.055 | 0.053 | 0.050 | 0.049 | 0.055 | 0.052 | 0.052 |
| s.d. | 0.007 | 0.007 | 0.006 | 0.006 | 0.005 | 0.004 | 0.006 | 0.003 | 0.003 |
| URI* | 0.087 | 0.101 | 0.083 | 0.084 | 0.082 | 0.078 | 0.100 | 0.086 | 0.088 |
| s.d. | 0.006 | 0.008 | 0.009 | 0.006 | 0.007 | 0.007 | 0.008 | 0.008 | 0.009 |
| BI | 0.889 | 0.858 | 0.889 | 0.881 | 0.852 | 0.892 | 0.746 | 0.877 | 0.858 |
| s.d. | 0.047 | 0.042 | 0.046 | 0.030 | 0.028 | 0.042 | 0.036 | 0.017 | 0.052 |
| Hindlimb | (n = 39) | (n = 29) | (n = 23) | (n = 11) | (n = 18) | (n = 33) | (n = 64) | (n = 152) | (n = 217) |
| FRI | 0.119 | 0.127 | 0.129 | 0.134 | 0.120 | 0.124 | 0.110 | 0.125 | 0.123 |
| s.d. | 0.009 | 0.014 | 0.013 | 0.013 | 0.013 | 0.017 | 0.010 | 0.006 | 0.008 |
| EIf | 0.239 | 0.262 | 0.257 | 0.300 | 0.279 | 0.264 | 0.240 | 0.267 | 0.263 |
| s.d. | 0.016 | 0.014 | 0.013 | 0.021 | 0.022 | 0.018 | 0.012 | 0.021 | 0.021 |
| FHI | 0.136 | 0.144 | 0.139 | 0.146 | 0.144 | 0.132 | 0.138 | 0.140 | 0.140 |
| s.d. | 0.010 | 0.007 | 0.007 | 0.011 | 0.008 | 0.007 | 0.012 | 0.006 | 0.005 |
| TSI | 0.491 | 0.483 | 0.456 | 0.468 | 0.445 | 0.425 | 0.388 | 0.461 | 0.451 |
| s.d. | 0.020 | 0.032 | 0.028 | 0.023 | 0.042 | 0.032 | 0.027 | 0.025 | 0.036 |
| TRI | 0.094 | 0.081 | 0.094 | 0.080 | 0.073 | 0.079 | – | 0.083 | – |
| s.d. | 0.006 | 0.008 | 0.010 | 0.007 | 0.008 | 0.009 | – | 0.009 | – |
| TRI* | 0.127 | 0.149 | 0.144 | 0.153 | 0.130 | 0.128 | – | 0.139 | – |
| s.d. | 0.012 | 0.019 | 0.009 | 0.018 | 0.014 | 0.013 | – | 0.012 | – |
| TJI | 0.599 | 0.531 | 0.517 | 0.547 | 0.533 | 0.529 | – | 0.543 | – |
| s.d. | 0.018 | 0.036 | 0.025 | 0.025 | 0.023 | 0.025 | – | 0.029 | – |
| CI | 0.927 | 0.987 | 0.979 | 1.035 | 1.059 | 1.067 | 1.028 | 1.009 | 1.012 |
| s.d. | 0.027 | 0.039 | 0.027 | 0.034 | 0.028 | 0.033 | 0.034 | 0.054 | 0.050 |
| IMI | 0.862 | 0.875 | 0.884 | 0.910 | 0.851 | 0.844 | 0.856 | 0.871 | 0.869 |
| s.d. | 0.030 | 0.024 | 0.026 | 0.030 | 0.023 | 0.019 | 0.019 | 0.024 | 0.023 |

Family mean values excluding *Heterocephalus glaber* are indicated with a double asterisk (**). See abbreviation of species and indices in Table 1, 2.

showed the statistically significant lowest values of HRI and BI in comparison to the rest of the bathyergids (Table 3 and Figure 3B).

The MANOVA including all indices (and excluding *H. glaber*) also showed significant differences among species [Wilks' $\lambda = 0.029$; $F_{(40, 726)} = 22.823$; $p < 0.001$]. High PES values were obtained only for IFA (0.588), although URI* (0.499) and RDT (0.409) also showed relatively high values (Table 4 and Supplementary Table 1). The rest of the variables (HRI, HHI, EIH, URI, and BI) showed low values (< 0.35), indicating that such variables do not contribute considerably to

species differentiation when the RDT index is included and *H. glaber* is absent (Table 4).

Pair-wise *post-hoc* tests showed significant differences between *H. glaber* and all other species for almost all indices, except for ulnar variables such as IFA, URI and URI* (Figure 3B). Thus, despite the functional length of the ulna (BI) of *H. glaber*, it appears relatively shorter as compared to other bathyergids, its general shape does not differ greatly from other species (Figure 3B). Only *B. suillus* showed a marked difference with the rest of the bathyergids, specifically the significantly lowest IFA values within the family (Table 3 and Figure 3B).

TABLE 4 MANOVAs on morpho-functional indices of the forelimb and hindlimb, including all species and all indices.

| | Test | Value | F | Hypothesis Df | Error Df | P | Partial eta squared (PES) | Indices (PES) > 0.50 |
|---------------------------------|----------------|-------|--------|---------------|----------|--------|---------------------------|----------------------|
| Forelimb (<i>all spp</i>) | Pillai's Trace | 2.469 | 23.580 | 42 | 1,416 | <0.001 | 0.412 | All except URI |
| | Wilks' Lambda | 0.013 | 38.961 | 42 | 1086.94 | <0.001 | 0.512 | |
| Forelimb (<i>all indices</i>) | Pillai's Trace | 2.251 | 17.396 | 40 | 850 | <0.001 | 0.450 | IFA |
| | Wilks' Lambda | 0.029 | 22.823 | 40 | 726.37 | <0.001 | 0.508 | |
| Hindlimb (<i>all spp</i>) | Pillai's Trace | 1.942 | 16.745 | 36 | 1,260 | <0.001 | 0.324 | EIF, TSI, CI |
| | Wilks' Lambda | 0.041 | 26.799 | 36 | 902.98 | <0.001 | 0.413 | |
| Hindlimb (<i>all indices</i>) | Pillai's Trace | 2.304 | 13.575 | 45 | 715 | <0.001 | 0.461 | EIF, TJI, CI |
| | Wilks' Lambda | 0.023 | 18.534 | 45 | 624.88 | <0.001 | 0.532 | |

Indices with high partial eta square (PES) values (> 0.50) are also presented (see all PES values in [Supplementary Table 1](#)).

This analysis showed that there are clear differences in the variable contribution of morpho-functional indices when *H. glaber* is included in the assessment. For example, the brachial index (BI) showed one of the highest PES values (0.697) when all species are analyzed, although showed one of the lowest values (0.139) when *H. glaber* is excluded ([Supplementary Table 1](#)). This indicates that some indices in *H. glaber* have a high explanatory power for species differentiation.

Multivariate analysis of the hindlimb

Since *H. glaber* does not exhibit a distal fusion of the tibia-fibula ([Figure 4A](#)), the TJI, TRI, and TRI* indices were not calculated for this species. Descriptive statistics of the morpho-functional indices are presented in [Table 3](#), and corresponding whisker plots in [Figure 4B](#). The MANOVA including all species showed significant differences among species [Wilks' $\lambda = 0.041$; $F_{(36, 902)} = 26.799$; $p < 0.001$] ([Table 4](#), [Figure 4B](#), and [Supplementary Table 1](#)). The highest PES values were found in EIF, TSI, and CI, while the rest of the indices showed quite low values (<0.33) ([Table 4](#) and [Supplementary Table 1](#)). The highest PES were in the tibia-fibula, the CI and TSI (0.686 and 0.667, respectively), for which *H. glaber* presented the significantly lowest TSI values among bathyergids ([Figure 4B](#)).

The MANOVA including all indices (and excluding *H. glaber*) also showed significant differences among species [Wilks' $\lambda = 0.023$; $F_{(45, 625)} = 18.534$; $p < 0.001$]. The indices with the highest PES values were CI (0.754), TJI (0.599), and EIF (0.507) ([Table 4](#)), so that the tibio-fibular indices contributed most to species differentiation. Contrary to the previous analysis, the TSI now showed lower values, thus indicating that for the tibio-fibula, the TSI does not contribute considerably to species differentiation. The high number of indices with high PES values in the hindlimb suggests more marked differences in the femur

and tibia of bathyergids in comparison to their forelimb bones ([Supplementary Table 1](#)). Tamhane *post hoc* tests showed only one significant difference between *H. glaber* and the other bathyergids, presenting the lowest TSI values, while *B. suillus* showed the highest and lowest values for TJI and CI, respectively, among bathyergids ([Figure 4B](#)).

In general, the MANOVAs (including all species) showed that the forelimb indices, particularly those associated with the humerus explain a greater proportion of the species differentiation as compared to the hindlimb indices when *H. glaber* is included in the analyzes.

Ordination analysis of the forelimb

The PCA that included all species (PCA_{F1}) generated six components, with most of the variation contained in the three first (98.28%), although most of this variation is explained by PC1, which contains 81.75% of the total variance ([Table 5](#) and [Figures 5A–C](#)). The indices that contributed most to the variation in PC1, following the criterion defined in previous studies, such as a high correlation between variables ($r^2 > 0.60$, [Wilson and Geiger, 2015](#)), were BI ($r^2 = 0.72$) and HRI ($r^2 = 0.62$) ([Supplementary Table 2](#)). Marked differences were observed in the morphospace occupied by *H. glaber* and the rest of the bathyergids along PC1. Most individuals and species were distributed in the positive side of PC1, showing both high BI and EI (Figure 5A), while *H. glaber* occupied a large area in the negative side of PC1 associated with a robust ulna (high URI and URI*). The PC2 represented only 11.56% of the total variation. The index that contributed most to the variation in this axis was the IFA ($r^2 = 0.82$) ([Supplementary Table 2](#)). Most specimens were equally distributed along the positive and negative sides of this axis, although the solitary species *B. suillus* and *He. argenteocinereus* tended to be associated with the extremes of the negative and positive sides, respectively. *Bathyergus suillus* tended to show

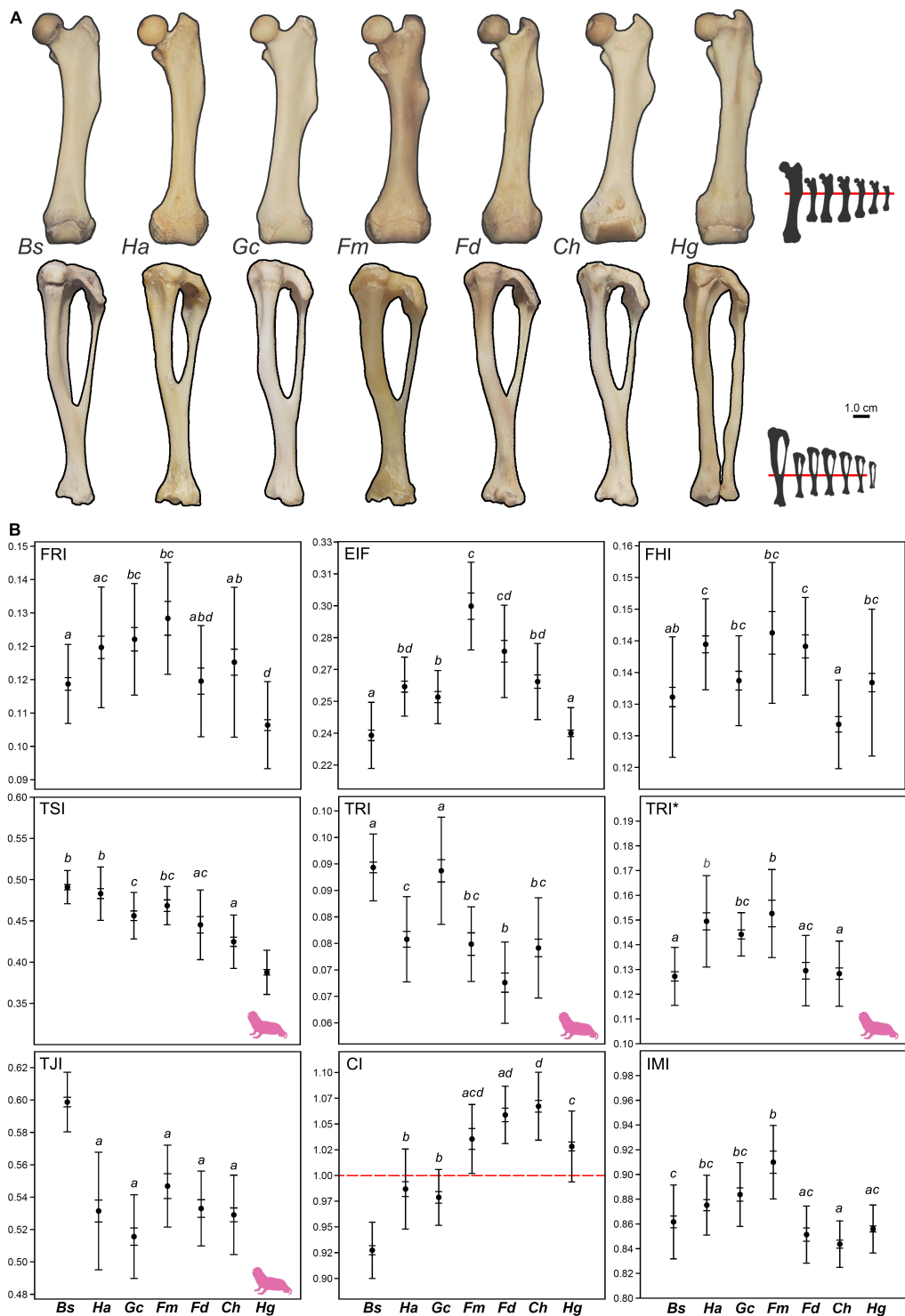


FIGURE 4
 Quantification of the hindlimb morphology (femur and tibia-fibula). **(A)** Femoral (top row) and tibio-fibular (bottom row) morphology of all species. Bones scaled to same size to emphasize differences in bone proportions. Small bones silhouettes show the real relative size of bones between species. The femora are aligned to the distal origin of the third trochanter, while the tibia-fibula are aligned to the distal tibio-fibular junction (except in *Heterocephalus glaber*). **(B)** Whisker plots showing differences among species. The red line in the crural index (CI) indicates symmetry (= 1) between femur and tibia-fibula. Mean (central point), s.e (short whiskers) and s.d. (long whiskers). Species that share the same letter represent homogeneous subsets, as identified by *post hoc* (Tamhane) tests. The pink silhouette represents *H. glaber* and indicates the indices for which this species differs significantly from other bathyergids, as well as the indices not measured for this species (i.e. lack of morphological specialization). Taxa ordered as in **Figure 3**. See abbreviation of indices in **Table 2**, and of species names in **Figure 3**.

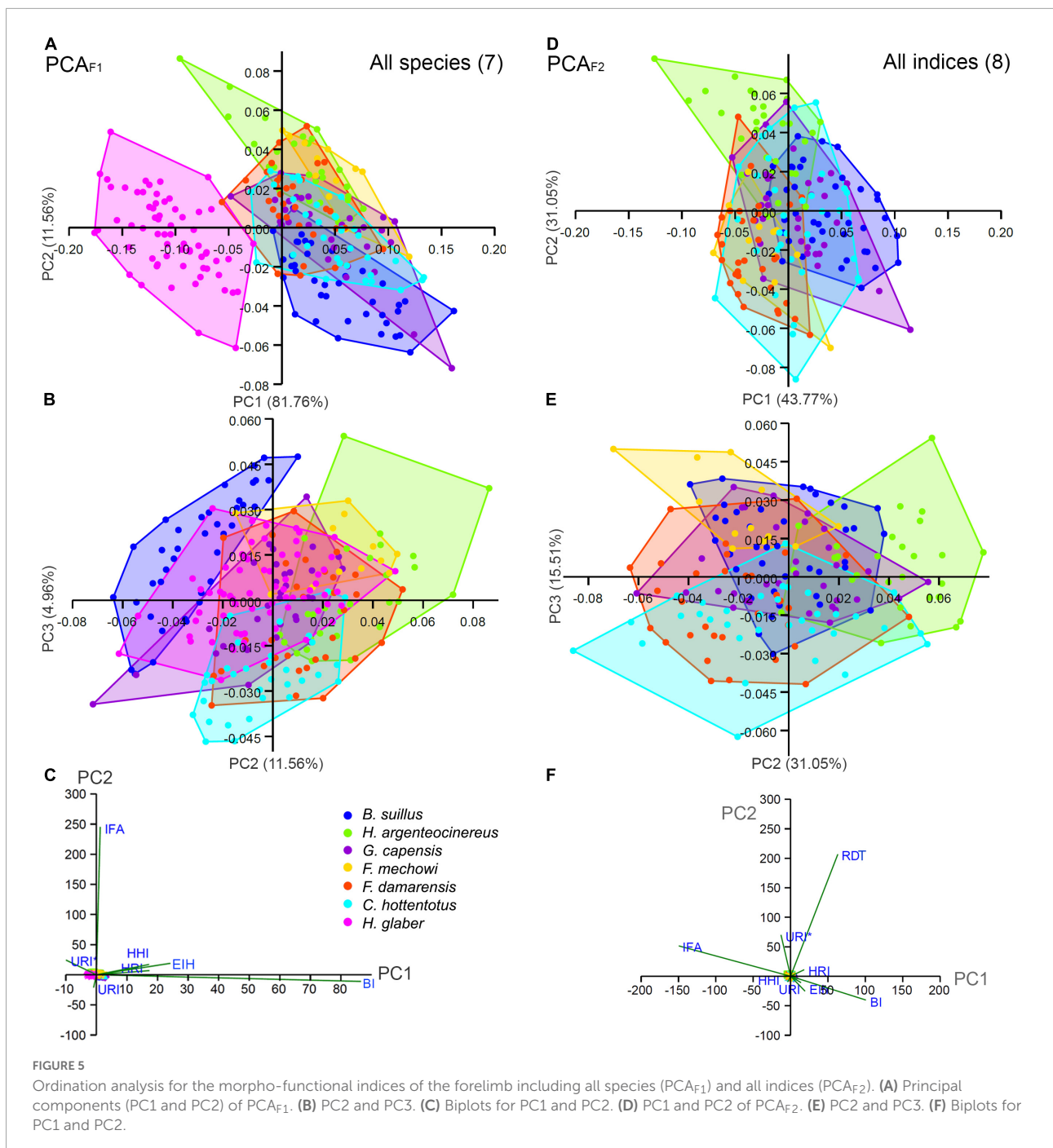
TABLE 5 Coefficients, eigenvalues, and proportion of variance for each principal component (PC) obtained for the analysis of forelimbs and hindlimbs, including all species (PCA_{F1} and PCA_{H1}) and all indices (PCA_{F2} and PCA_{H2}).

| Indices | PC 1 | PC 2 | PC 3 | PC 4 | PC 5 | PC 6 |
|--|--------|--------|--------|--------|--------|--------|
| Forelimb—All species (PCA_{F1}) | | | | | | |
| HRI | 0.185 | 0.028 | 0.277 | 0.294 | 0.136 | 0.765 |
| HHI | 0.184 | 0.068 | -0.336 | 0.094 | 0.859 | 0.068 |
| EIH | 0.258 | 0.076 | 0.834 | -0.274 | 0.284 | -0.262 |
| IFA | 0.013 | 0.985 | -0.070 | -0.090 | -0.113 | 0.057 |
| URI | -0.010 | -0.085 | 0.129 | -0.149 | -0.253 | 0.518 |
| URI* | -0.106 | 0.098 | 0.238 | 0.888 | -0.070 | -0.236 |
| BI | 0.924 | -0.044 | -0.192 | 0.101 | -0.287 | -0.116 |
| Eigenvalue | 0.003 | 0.000 | 0.000 | 0.000 | 0.000 | 0.000 |
| % Variance | 81.758 | 11.560 | 4.959 | 0.938 | 0.758 | 0.027 |
| Forelimb—All indices (PCA_{F2}) | | | | | | |
| RDT | 0.326 | 0.899 | -0.010 | 0.059 | 0.026 | |
| HRI | 0.094 | 0.048 | 0.283 | -0.097 | 0.027 | |
| HHI | -0.020 | -0.043 | -0.290 | -0.018 | 0.858 | |
| EIH | 0.100 | -0.110 | 0.846 | -0.219 | 0.290 | |
| IFA | -0.772 | 0.224 | 0.240 | 0.531 | 0.041 | |
| URI | 0.072 | -0.047 | 0.108 | -0.022 | -0.399 | |
| URI* | -0.067 | 0.305 | 0.172 | -0.180 | 0.101 | |
| BI | 0.519 | -0.175 | 0.145 | 0.790 | 0.086 | |
| Eigenvalue | 0.001 | 0.000 | 0.000 | 0.000 | 0.000 | |
| % Variance | 43.773 | 31.050 | 15.510 | 8.745 | 0.923 | |
| Hindlimb—All species (PCA_{H1}) | | | | | | |
| FRI | -0.029 | 0.196 | 0.038 | -0.697 | 0.280 | 0.629 |
| EIF | 0.136 | 0.569 | 0.025 | 0.230 | -0.675 | 0.384 |
| FHI | -0.005 | 0.101 | 0.066 | 0.672 | 0.574 | 0.453 |
| TSI | -0.493 | 0.560 | -0.578 | -0.017 | 0.194 | -0.267 |
| CI | 0.848 | 0.314 | -0.215 | -0.076 | 0.261 | -0.248 |
| IMI | -0.134 | 0.463 | 0.783 | -0.064 | 0.174 | -0.346 |
| Eigenvalue | 0.003 | 0.001 | 0.000 | 0.000 | 0.000 | 0.000 |
| % Variance | 67.706 | 24.902 | 6.727 | 0.491 | 0.134 | 0.040 |
| Hindlimb—All indices (PCA_{H2}) | | | | | | |
| FRI | 0.016 | 0.161 | -0.044 | 0.134 | 0.385 | |
| EIF | 0.223 | 0.408 | 0.318 | -0.028 | -0.488 | |
| FHI | 0.007 | 0.135 | 0.050 | -0.277 | -0.446 | |
| TSI | -0.335 | 0.274 | 0.223 | -0.689 | 0.193 | |
| TRI | -0.319 | -0.232 | 0.847 | 0.252 | 0.146 | |
| TRI* | -0.070 | 0.735 | 0.066 | 0.435 | -0.002 | |
| TJI | 0.847 | -0.030 | 0.314 | -0.083 | 0.258 | |
| CI | -0.003 | 0.347 | -0.099 | -0.130 | 0.538 | |
| IMI | -0.112 | -0.007 | -0.119 | 0.393 | 0.000 | |
| Eigenvalue | 0.004 | 0.001 | 0.001 | 0.000 | 0.000 | |
| % Variance | 70.527 | 17.618 | 9.536 | 2.014 | 0.305 | |

relatively low IFA values, while *He. argenteocinereus* high values.

The second PCA including all indices, and excluding *H. glaber* (PCA_{F2}) generated five components, with most of the variance contained in the four first components

(99.08%) (Table 5 and Figures 5D,E). Species distribute almost evenly in the center of the two first components (74.82%). The main contributor to PC1 (43.77%) was IFA ($r^2 = 0.76$) (Supplementary Table 2). Most species share both positive and negative values indicating

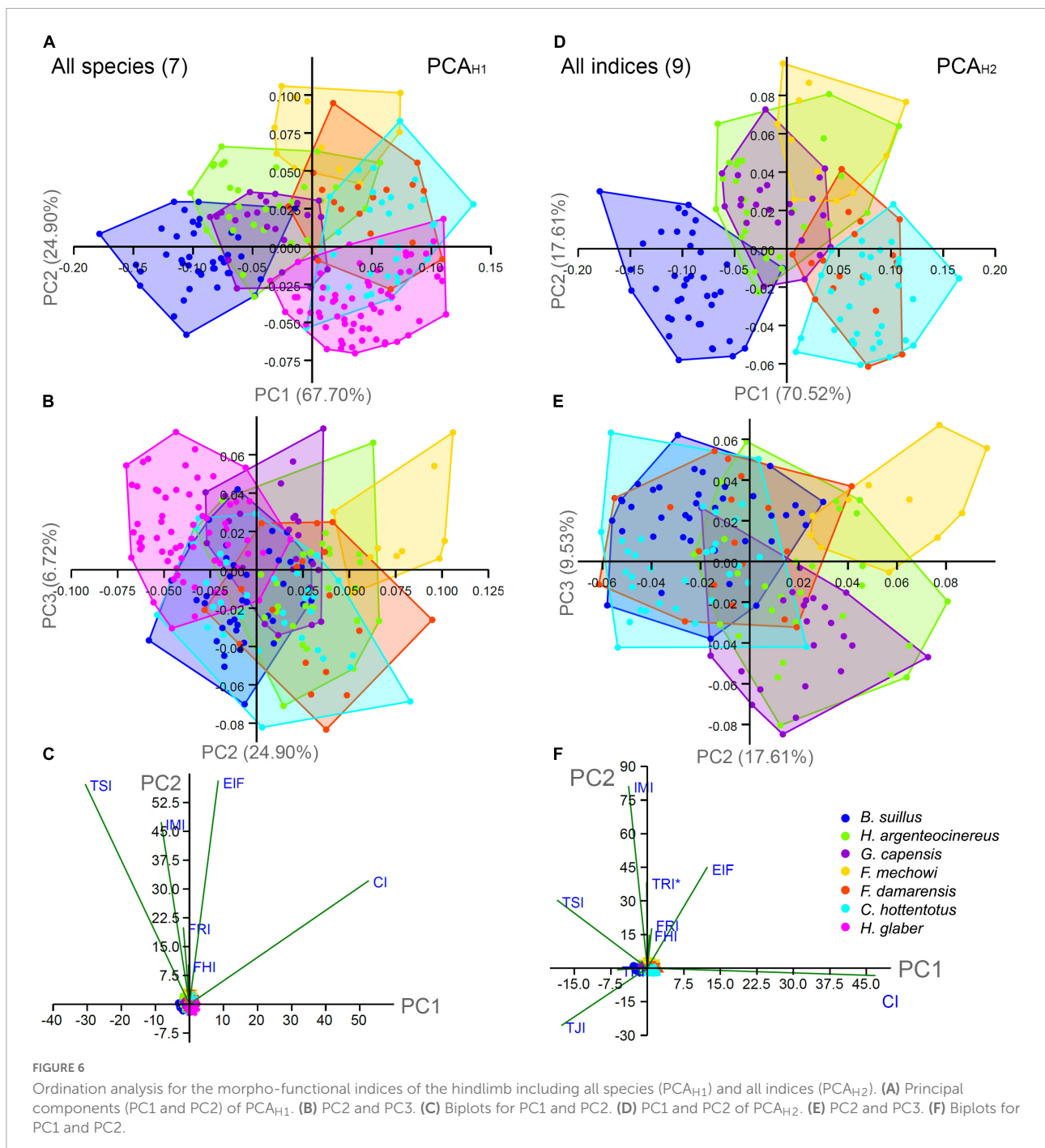


intermediate IFA values and only *B. suillus* positioned mostly in the positive side of PC1, thus indicating relatively lower values for IFA. *Fukomys* spp. and *He. argenteocinereus* tended to have higher IFA values. The main contributors to PC2 (31.05%) were RDT ($r^2 = 0.68$) and URI* ($r^2 = 0.67$) (Supplementary Table 2), which were mostly associated with the positive side of the axis. Only *He. argenteocinereus* and *F. mechowii* distributed either in the positive and

negative sides of the axis, respectively, whereas all the other species showed an intermediate distribution in the axis.

Ordination analysis of the hindlimb

The PCA including all species (PCA_{H1}) generated six components where the three first explained 99.33% of the



variance (Table 5 and Figures 6A–C). The PC1 represented 67.71% of the total variance, and it was able to separate *B. suillus* from all other social species, although not able to completely separate it from *He. argenteocinereus* and *G. capensis*. The CI showed the highest contribution ($r^2 = 0.85$), although TSI also showed high contribution ($r^2 = 0.57$) in this axis. Individuals of solitary species distributed mostly in the negative side of PC1, and were associated with higher TSI index, while the social species mostly occupied the positive side of the axis

only and were associated with a higher CI index. The PC2 (25.90%) was able to differentiate between the largest social species (*F. mechowii*) in the positive side and the smallest social species (*H. glaber*) in the negative side, with the exception of a few individuals (Figure 6A). The PC2 is mainly associated with increased EIF, FRI and IMI, although EIF showed the highest correlation ($r^2 = 0.87$). Thus, *F. mechowii* showed higher EIF, TSI, and IMI as compared to *H. glaber*. The largest bathyergid, *B. suillus* distributed evenly on both sides

of the axis, being intermediate between *F. mechowii* and *H. glaber*.

The second PCA including all indices (PCA_{H2}) generated five components where the three first explained 97.68% of the total variance (Table 5 and Figures 6D,E). The PC1 (70.53%) was positively correlated with CI ($r^2 = 0.86$) and EIF ($r^2 = 0.61$), and negatively correlated with TRI ($r^2 = 0.62$) (Supplementary Table 2). Social species distributed mostly in the positive side of this axis, while the negative side was mostly occupied by solitary species. *Bathyergus suillus* showed higher TSI and TJI as compared to other species. The other solitary species (*He. argenteocinereus* and *G. capensis*) occupied an intermediate position between *B. suillus* and social species (Figures 6D–F). The PC2 contributed only with 17.62% of the variance and the greatest positive correlations were obtained for IMI ($r^2 = 0.75$) and TRI* ($r^2 = 0.64$) (Supplementary Table 2). In this axis, *F. mechowii* occupied the positive sector, while most individuals of *C. hottentotus* (the second smaller species in this study) occupied the negative sector. In this sense, *F. mechowii* showed higher IMI and TRI* as compared to *C. hottentotus* and *B. suillus*.

Discriminant analysis (forelimb and hindlimb)

The LDA₁ (all species) showed a significant separation between groups [Wilks' $\lambda = 0.063$; $F_{(26, 402)} = 45.72$; $p < 0.001$], and the variables that most contributed to such discrimination (i.e., variables with the largest standard deviation) were BI, CI, TSI, and IFA. Two canonical functions were obtained, from which the first function (DF1) accounted for 86.81% of the variance, and was positively correlated with BI and TSI, and negatively correlated with CI (Table 6 and Figure 7A). The second function (DF2) accounted for 13.19% of the variance, and was also positively correlated with BI and TSI, and negatively correlated with IFA. All individuals in the scratch-digging group and many of the solitary chisel-tooth digger group were on the positive side of DF1, reflecting a trend for longer functional ulna (BI), larger tibial tuberosity (TSI), and shorter tibia in relation to the femur (CI). The rest of the individuals in the solitary chisel-tooth digger group, whereas most of the social chisel-tooth diggers were on the negative side, mainly indicating a larger tibia (CI) (Figure 7A). The DF2 separated most solitary chisel-tooth diggers on the positive side from most of the scratch-diggers in the negative side, indicating a larger olecranon (IFA) in solitary chisel-tooth diggers. Jackknifed cross-validation of group assignments produced a 93.06% of correctly classified individuals (Supplementary Table 3). In the scratch-digging group, all individuals were correctly classified. The solitary chisel-tooth diggers and social chisel-tooth diggers groups were not completely separated by the analysis; 15 individuals (6.94%) were misclassified. Most

TABLE 6 Loadings, eigenvalues, and proportion of variance explained by each function of the discriminant analysis, including all species (LDA₁) and all indices (LDA₂).

| Indices | Loadings | |
|--------------------------------------|----------|---------|
| | DF1 | DF2 |
| LDA₁ (All species) | | |
| HRI | 32.555 | 1.564 |
| HHI | -0.069 | -14.316 |
| EIH | 39.250 | -21.578 |
| IFA | -25.404 | 52.713 |
| URI | -27.326 | 14.961 |
| URI* | 17.591 | 40.070 |
| BI | 3.799 | 20.380 |
| FHI | 23.022 | 36.098 |
| FRI | -11.049 | 3.388 |
| EIF | -40.133 | -4.540 |
| TSI | 11.116 | -5.465 |
| CI | -19.187 | -8.105 |
| IMI | -7.965 | 9.263 |
| Eigenvalue | 6.737 | 1.024 |
| % | 86.810 | 13.190 |
| LDA₂ (All indices) | | |
| RDT | -6.280 | 12.595 |
| HRI | -31.797 | 13.908 |
| HHI | 9.433 | -14.700 |
| EIH | -40.159 | -18.942 |
| IFA | 52.712 | 36.691 |
| URI | 17.597 | 8.433 |
| URI* | -33.044 | 34.425 |
| BI | 10.076 | 15.153 |
| FHI | -31.999 | 86.971 |
| FRI | 19.414 | 0.427 |
| EIF | 47.882 | -11.748 |
| TSI | -7.540 | -0.727 |
| TRI | -1.809 | -0.580 |
| TRI* | -7.128 | -31.353 |
| TJI | -8.965 | -34.811 |
| CI | 10.419 | -22.708 |
| IMI | 4.092 | 6.615 |
| Eigenvalue | 9.266 | 2.569 |
| % | 78.290 | 21.710 |

misclassifications (11) were found within the social chisel-tooth digger group, where several specimens of *F. mechowii* were misclassified as solitary chisel-tooth diggers. None of the individuals in the analysis were misclassified as scratch-diggers and none of the individuals of *H. glaber* were misclassified.

The LDA₂ (all indices) also showed a significant separation between groups [Wilks' $\lambda = 0.027$; $F_{(34, 266)} = 39.53$; $p < 0.001$], and the variables that most contributed to such discrimination were CI, TSI, TJI, IFA, and IMI. Two canonical functions

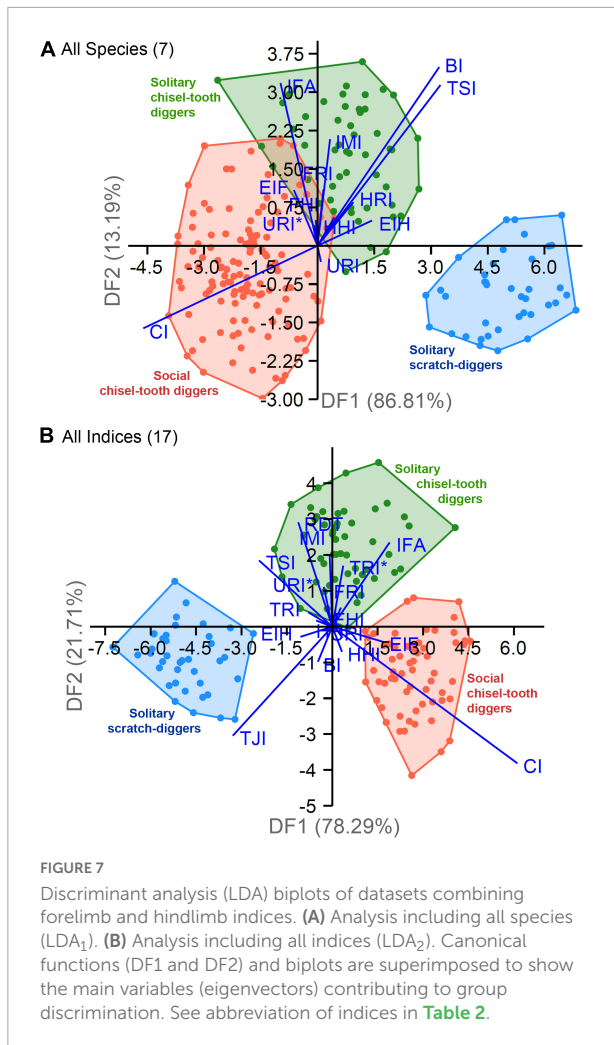


FIGURE 7
Discriminant analysis (LDA) biplots of datasets combining forelimb and hindlimb indices. (A) Analysis including all species (LDA₁). (B) Analysis including all indices (LDA₂). Canonical functions (DF1 and DF2) and biplots are superimposed to show the main variables (eigenvectors) contributing to group discrimination. See abbreviation of indices in **Table 2**.

were obtained, from which the first function (DF1) accounted for 78.29% of the variance, and was positively correlated with CI, and negatively correlated with TSI and TJI (**Table 6** and **Figure 7B**). All individuals of the scratch-digging group were associated with the negative side of DF1, indicating a trend for a larger tibial spine (TSI), shorter tibio-fibular fusion area (TJI), and shorter tibia (CI) as compared to the other groups. Social chisel-tooth diggers occupied the positive side of DF1, while solitary chisel-tooth diggers occupied both sides of the DF1. The second function (DF2) accounted for 21.71% of the variance, and was negatively correlated with IFA and IMI, and negatively correlated with CI (**Table 6**). The exclusion of *H. glaber* allowed a clear separation between social and chisel-tooth diggers. Solitary chisel-tooth diggers were on the positive side of DF2, indicating a trend for larger olecranon process (IFA), larger tibia, and longer hindlimb proportions (IMI), while the other two groups a trend for shorter tibia (CI) and smaller tibio-fibular fusion area (TJI). Jackknifed cross-validation produced a 97.37% of correctly classified individuals (**Supplementary Table 3**). As in LDA₁, all specimens in the

first group were correctly classified, although only 4 individuals (0.97%) (mostly pertaining to the solitary chisel-tooth digger group) were misclassified. This represents a considerably low number of misclassifications, probably related to the inclusion of additional indices (i.e., RDT, TRI, TRI*, and TJI), which showed significant explanatory power in previous multivariate analyses (**Tables 3–5**). Thus, the inclusion of humeral and tibio-fibular indices in LDA₂ represents a 4.31% increment in discriminant power respect to LDA₁. It is likely that the exclusion of *H. glaber* from LDA₂ also contributed to a better discrimination between groups, since this species showed a highly variable forelimb and hindlimb morphology, which overlap other species (**Figure 5**).

Sex differences

Only two species exhibited significant sex differences in BM, *B. suillus* and *F. damarensis* (**Supplementary Table 4**), although no statistical differences were detected for morpho-functional indices for most bathyergids (**Supplementary Table 5**), as well as for *H. glaber* ($U = 0.560$; $p = 0.715$).

Discussion

The multivariate analysis of morpho-functional indices of the humerus, ulna, femur and tibia-fibula of all bathyergid genera including seven species showed significant differences within the family, although no significant differences between sexes. *Heterocephalus glaber* showed the highest level of morphological disparity in the family, lacking several discrete features. Because of the high level of disparity of *H. glaber*, the following discussion focuses firstly on the main differences among bathyergids, while the functional anatomy of naked mole-rats is treated separately in the next section.

One of the most remarkable findings of this study is that several forelimb indices appeared equally or more specialized in chisel-tooth diggers (including social species) rather than in the scratch-digger species, which do not agree with our initial expectations. Chisel-tooth diggers presented highly developed fossorial features like those of specialized scratch-diggers: including a prominent deltoid tuberosity, enlarged olecranon process, and fused tibia-fibula (**Lehmann, 1963; Hildebrand, 1985; Samuels and Van Valkenburgh, 2008; Steiner-Souza et al., 2010**). This suggests that despite their primary digging mode, their limb anatomy is also under strong selection for burrowing (see also **Montoya-Sanhueza et al., 2022a**). Some well-developed indices observed in chisel-tooth diggers were the olecranon process (IFA), the anteroposterior robustness of the ulna (URI*) and the relative position of the deltoid tuberosity (RDT) (**Figure 3** and **Supplementary Table 1**). Similar results were obtained from the ordination analysis of the forelimb, where IFA and RDT contributed greatly to separate species and

ecomorphological groups (Figures 5F, 6F, 7B). A high IFA index reflects a relatively larger olecranon process of the ulna, and consequently indicates larger areas for the attachment of the *mm. triceps brachii* and *m. epitrochlearis*. These muscles are directly related to elbow extension for generation of stronger mechanical advantage, hence is a good estimator of the parasagittal scratch-digging ability in mammals (Vizcaíno et al., 1999, 2016). The highest IFA values were observed in the solitary chisel-tooth digger *He. argenteocinereus*, which also showed the most distally located deltoid tuberosity (RDT) and thickest anteroposterior diameter of ulna (URI*) (Table 3 and Figure 3). The largest social bathyergid, *F. mechowii* also showed a large olecranon process. These results are unexpected since *Heliophobius* and *Fukomys* are primarily chisel-tooth diggers that use their forelimbs secondarily for burrow construction (e.g., Jarvis and Sale, 1971; Van Wassenbergh et al., 2017). Although, *Bathyergus* is the only scratch-digger of the family which uses primarily its long fore-claws for breaking up the soil (Davies and Jarvis, 1986), it showed the lowest IFA values, thus having a comparatively shorter olecranon process (Figure 3). A high URI* reflects a relatively thicker anteroposterior cross-sectional shape of the ulna and an increased mechanical advantage for resisting bending strains, thus reducing fracture risks during burrowing (Montoya-Sanhueza et al., 2019, and references therein). This may also increase the area available for the attachment of muscles involved in pronation and supination of the forearm, and flexion of the manus and digits, important for scratch-digging. The highest URI* values were found in *He. argenteocinereus* (and *H. glaber*), allowing them sustain higher strains during parasagittal scratch-digging (Figure 3). The projected and distally located deltoid tuberosity (RDT) is other important trait characterizing highly specialized fossorial mammals, since is principally adapted to accommodate enlarged *mm. pectorales* and *mm. deltoidei*, thus increasing the in-lever ability and power-stroke (flexion/retraction) of the arm (Hildebrand, 1985; Álvarez et al., 2012). The more distally located deltoid tuberosity was observed in *He. argenteocinereus*, and indicates a stronger flexion of the humerus, and therefore a stronger ability of the forelimb for pulling the substrate out against the body. In general, all solitary species (and the social *C. hottentotus*) showed a more distal location of this feature as compared to the highly social species of genus *Fukomys*, with *B. suillus* showing an intermediate level (Figure 3).

A similar pattern was observed for hindlimb indices, where chisel-tooth diggers exhibited equally similar or higher indices as compared to *B. suillus*. In general, the indices that most contributed to species differences were associated with the tibia-fibula, like the tibio-fibular fusion (TJI), mediolateral diameter of the diaphysis (TRI), size of the tibial spine (TSI), and size of the tibia-fibula in relation to the femur (CI). In the femur, only the size of the epicondyles (EIF) contributed most to interspecific differences (Figure 4). Among these indices, the TJI, TSI, and EIF were equally developed or more specialized

in chisel-tooth diggers than in *B. suillus*. The TJI reflects the degree of distal fusion between tibia and fibula, and represents a novel index to assess the robustness of the hindleg. The fused (ossified) condition is found in burrowing or swimming animals that use their hindlimbs in action against a resistant medium such as earth or water, and this contrasts with the condition of many terrestrial and arboreal mammals where the fibula remains separated, and is relatively mobile to increase agility and the range of limb/pes motion (Carleton, 1941; Moss, 1977; Stein, 2000). Larger fusion areas would increase the resistance for bending and torsional loads imposed by strong pulling of muscles, which may be advantageous in fossorial animals. Apart from *H. glaber*, which lacks an ossified tibio-fibular fusion, most bathyergids showed a larger fusion area as compared to *B. suillus* (Figure 4), suggesting that larger body sizes may not determine the ossification of such bones. The TSI reflects the strength of the leg and the relative width available for the insertion of the *m. semitendinosus* and *m. semimembranosus* in the tibial spine, so that wider surface areas increase the in-lever action to retract muscles and hence increase the strength of the knee (Samuels and Van Valkenburgh, 2008). A larger tibial spine was found in large bathyergids (e.g., *B. suillus*, *G. capensis* and *F. mechowii*), while the lowest values occurred in the smaller species (e.g., *C. hottentotus* and *H. glaber*) (Figure 4). A similar trend was found by Sahd et al. (2020), with *B. suillus* having higher TSI (0.491) as compared to *C. h. natalensis* (0.422). This relationship suggests a positive trend with body size, a pattern that was also reported among caviomorph rodents with different digging capabilities (Elissamburu and Vizcaíno, 2004). The EIF indicates the relative area available for the origin of the *m. gastrocnemius* used in the flexion of the knee and ankle. The larger epicondyles among bathyergids were found in social taxa, especially in *F. mechowii*, with solitary species showing relatively narrower epicondylar widths (Figure 4). Similar qualitative observations have been reported by Sahd et al. (2019), where the epicondyles of the social *C. h. natalensis* appeared more robust and prominent as compared to the solitary species *B. suillus* and *G. capensis*, although posterior quantification showed similar high values between *C. h. natalensis* and *G. capensis* (Sahd et al., 2020).

Because of its primary digging mode, the long bones of *B. suillus* are expected to generate stronger forces and undergo higher mechanical strains during elbow extension as compared to chisel-tooth diggers, therefore their limbs were expected to exhibit higher bone robustness and fossorial ability. Although *B. suillus* exhibited high specialization for several indices, these were not significantly higher than chisel-tooth diggers. This does not support our hypothesis of higher functional specializations in bathyergid scratch-diggers, and rather suggests an “equally” important role of limbs for digging in chisel-tooth diggers. This does not imply that chisel-tooth diggers actually use primarily their claws and forelimbs for loosening soils. Actually, the claws of the pes and manus of these chisel-tooth diggers are significantly reduced as compared to *Bathyergus* (Figure 1),

with *C. hottentotus*, *He. Argenteocinereus*, and *H. glaber* rather showing a lower claw length index as compared to other fossorial rodents (see Samuels and Van Valkenburgh, 2008). This suggests that more specialized limbs (stylopods and zeugopods) in chisel-tooth diggers may be advantageous for other phases of the digging process. For example, the generation of forward forces for biting soils, shoulder/neck support, body support, and transporting/removing soils out of the burrows may be equally or energetically more demanding tasks as compared to breaking up soils solely (see below), and therefore undergo high selective pressures. Similarly, since several indices were equally, or more developed in social species, our results neither support the hypothesis of lower specialization in social species as compared to solitary ones due to sharing the costs of burrowing. Although the LDA (excluding *H. glaber*) was able to significantly discriminate ecomorphological groups and characterize solitary chisel-tooth diggers from social chisel-tooth diggers by having increased IFA, RDT, and TSI (Figure 7B), this only represents a 21.71% of the variance in the sample.

An explanation for such high levels of specialization in mole-rats with different digging modes may lie with the substrates these species occupy. The relatively smaller olecranon of *B. suillus* may be associated with the soft soils in which this species lives, mostly composed of loose sandy soils (Davies and Jarvis, 1986; Bennett et al., 2009), in comparison with the much harder soils (clays and loams) occupied by chisel tooth-diggers (e.g., Bennett et al., 1988; Bennett and Faulkes, 2000; Šumbera et al., 2008, 2012; Lövy et al., 2012). Living in such soft substrate conditions could reduce the energetic requirements of digging (Vleck, 1979; Luna and Antinuchi, 2006; Zelová et al., 2010), and therefore preclude higher specialization. In this respect, important advances on the understanding of the digging habits and the postcranial morphology of subterranean mammals have been done in the South American tuco-tucos of the rodent family Ctenomyidae (Vassallo, 1998; Steiner-Souza et al., 2010; Vassallo et al., 2021). Several studies have found a more specialized (e.g., robust) humeral and cranial morphology in *Ctenomys* species inhabiting harder soils, whereas a more slender humeral morphology in species inhabiting softer soils (e.g., Steiner-Souza et al., 2010). In particular, Vassallo (1998) found that *Ctenomys talarum*, a species living in hard soils exhibits relatively larger *mm. triceps brachii* as compared to *Ct. australis*, which lives in sandy and friable soils. Because the triceps group inserts into the olecranon process, these muscles are directly associated with the generation of greater out-forces during scratch-digging (Vassallo, 1998), and consequently a larger olecranon may represent an important feature in chisel-tooth digging mole-rats to compensate for burrowing in harder substrates. Similar observations have also been reported for intraspecific assessments among populations of *Ct. minutus* living in different habitat types (and soil hardness); the population living in softer soils has a less specialized skull morphology, humeral morphology, as well as estimators of

bite force as compared to the population living in harder soils (Kubiak et al., 2018). Among bathyergids, Barčiová et al. (2009) also suggested that the morphological variations in skull morphology (e.g., relatively shorter rostrum) found in different populations of *He. argenteocinereus* may be related to differences in soil parameters between localities (e.g., soil hardness), and Kraus et al. (2022) revealed how habitat characteristics are responsible for high bite force across different mole-rat species.

Overall, the above information indicates that burrow construction in harder soils imposes stronger constraints on limbs (e.g., ulna and tibia-fibula), so that such species may require increased limb specialization as species living in softer soils, even when they are primarily chisel-tooth diggers. Stronger ulnar flexion in chisel-tooth diggers may be beneficial in environments where the soils may reach a high degree of compaction and/or become heavier due to changes in soil properties, such as increased moisture during the rainy seasons. For example, the net cost of transporting soils depends on several parameters, including moisture content, soil density, adhesion and viscosity among others (Vleck, 1979; Luna and Antinuchi, 2006). When soils are wet, particularly during the rainy seasons, these increase considerably their mass and viscosity (Collis-George, 1959; Marcy et al., 2013), making its excavation more demanding. Recent assessments on the effects of soil compactness on burrowing performance in talpid moles indicate that increased soil compactness impedes tunneling performance, resulting in reduced burrowing speed, shorter tunnels, shorter activity time and less time spent burrowing continuously (Lin et al., 2017). Moreover, the successive components of the entire burrowing sequence are most likely not energetically equivalent, and some activities such as pushing off of the soils along the tunnel and throwing it out may represent the most energy-consuming phase during the entire burrowing process (Gambaryan and Gasc, 1993). In fact, the estimations of the energy costs of burrowing in pocket gophers (Vleck, 1979) and tuco-tucos (Luna et al., 2002) have shown that although the cost of breaking the soil (shearing) is *per se* energetically higher than transporting it (pushing), the transport phase represents a considerably longer process (in terms of time), hence increasing its total costs throughout the entire burrow construction. In African mole-rats, above-ground digging activity has been associated with seasonality (Jarvis et al., 1998; Bennett and Faulkes, 2000), suggesting that overall digging activity increases during the rainy season, since soils are easier to loosen as compared to the more compacted soils of the dry season. Therefore, it is possible that both the transport and removal of soils out of the tunnels represents energetically demanding activities in Bathyergidae, so the forelimb and hindlimb undergo strong selective pressures and increased specialization, regardless of their primary digging mode. Indeed, such level of limb specialization in chisel-tooth diggers is in concordance with their augmented dental and cranial specializations adapted to breaking up harder substrates

(McIntosh and Cox, 2016a). Although the evolution of a highly specialized chisel-tooth digging apparatus in bathyergids may be highly associated with the exploitation of harder soils (McIntosh and Cox, 2016a), it is known that chisel-tooth diggers can occupy a wide range of habitats including softer substrates, e.g., *F. damarensis* (Bennett and Jarvis, 2004; Lövy et al., 2012; Thomas et al., 2016). This suggests that there are no strong apparent ecological constraints on chisel-tooth mole-rats to occupy a diverse range of habitats and soil conditions, which is most likely promoted not only by the extreme specialization of their cranial and dental anatomy, but also by their highly specialized appendicular morphology.

Locomotion

Three indices (CI, BI, IMI) reflect important aspects associated with locomotion. In particular, the CI gives an indication of how well the hindlimbs are adapted for speed (Howell, 1965), and it showed an important amount of variation among species. The lower CI values (i.e., shorter tibia-fibula in comparison to the femur) were found in solitary species, while the higher values (i.e., larger tibia-fibula) were found in social species, especially in the smaller ones (*F. damarensis* and *C. hottentotus*) (Table 3 and Figure 4B). Longer zeugopods are typically found in surface-dwelling mammals, particularly in cursorial ones (Howell, 1965), although the social bathyergids still showed lower values as compared to surface-dwelling species (Samuels and Van Valkenburgh, 2008). This suggests that social species may have faster propulsive forces as compared to solitary species, allowing the capacity for faster movements and locomotion. Apart from indicating leaping ability in particular cases like saltatorial mammals, the IMI has not shown clear functional correlates in mammals, especially those associated with either higher speed or lack of it (Howell, 1965). This author reported an IMI of 0.75 as the generalized condition for large terrestrial mammals, so that the hindleg is longer than the foreleg, with bipedal jumpers showing the lowest ratios (0.32–0.50). Bathyergids have higher IMI values (0.87) as compared to terrestrial mammals, thus evidencing relatively symmetrical limb proportions, although the hindlimb is still slightly longer than the forelimb (Figure 4). Lehmann (1963) also found that the length of the hindlimbs of the fossorial *Geomys*, *Ctenomys*, and *Tachyoryctes* are nearly equal to the length of the forelimbs, differing from non-fossorial forms like *Rattus*, in which there is a tendency for the hindlimbs to be longer. This high interlimb symmetry is also related to the similar proportion between humerus and ulna (BI), although it is probable that by adding the scapular length to the length of the forelimb, as other studies have suggested (e.g., Lilje et al., 2003), the IMI ratio would change, making the proportions in bathyergids even more symmetrical. Montoya-Sanhueza et al. (2019) described

the limb development of *B. suillus* and discussed the function of symmetric limb proportions in subterranean mammals, suggesting that symmetrical limb proportions may be related to maximizing equal bidirectional locomotion within burrows by emphasizing equal propulsive action of the forelimbs and hindlimbs, without changing body posture and orientation (Eilam et al., 1995). Overall, the high IMI of bathyergids and other fossorial mammals, along with their usually short limbs, may not represent a fossorial adaptation for excavation *per se*, but a morphological specialization for bidirectional locomotion in narrow spaces and a dense medium (Howell, 1965; Eilam et al., 1995). Although the locomotory dynamics of bathyergids have not been assessed, these characteristics may compromise the locomotor capabilities of mole-rats in comparison to terrestrial mammals (Howell, 1965; Samuels and Van Valkenburgh, 2008). Montoya-Sanhueza et al. (2019) pointed out the apparent lower locomotor capabilities of *B. suillus* in comparison to the ctenomyid *Ct. talarum*, which suggests that living underground not always results in reduced locomotor capabilities. Further research on locomotory dynamics of subterranean mammals, would help us understand the relationship between morphology and locomotion in this particular ecomorphological group of mammals.

The limb phenotype of *Heterocephalus glaber*: Functional implications

The limb anatomy of *H. glaber* lacks two important discrete fossorial limb adaptations, the projected deltoid tuberosity and distal tibio-fibular fusion (Montoya-Sanhueza et al., 2022a). This precluded the measurement of RDT, TRI, TRI*, and TJI. However, *H. glaber* accumulated most of the interspecific differences in morpho-functional indices in the family (Figures 3, 4). Out of seven forelimb indices, four were significantly different in *H. glaber*, showing a comparatively less robust humeral diaphysis (low HRI), smaller humeral head (low HHI), narrower epicondyles (low EIH) and “shorter ulna” (functional length, without olecranon process) as compared to the humerus (low BI) (Table 3 and Figure 3). Because the different morphology of the humeral diaphysis in *H. glaber*, a slightly different calculation for the HRI was also obtained, making comparisons not straightforward among bathyergids. In most species, the HRI was measured around 58–60% the length of the humerus from the proximal epiphysis (because the presence of the deltoid tuberosity), although in *H. glaber* this was taken at 50% of the total length. This represents a more proximal measurement as compared to the other bathyergids, however because of the even thinner morphology of the humerus at lower locations (e.g., 58–60%) in *H. glaber*, a comparable measurement with other bathyergids would result in even thinner estimations. Related to this section of the

bone, the cross-sectional shape of the humerus at 50% of the bone length in bathyergids is strongly influenced by the deltoid tuberosity, resulting in a rather triangular shape. This section in *H. glaber* is more elongated and ellipsoidal (see Montoya-Sanhueza et al., 2021a), thus probably compensating for the lack of a prominent tuberosity. Yet, the diaphysis of *H. glaber* is considerably thinner as compared to other bathyergids. Regarding the low BI, several individuals of *H. glaber* showed a curved ulna, which may explain the low values of this index. Although *H. glaber* (and *He. argenteocinereus*) showed the highest URI* among bathyergids, reflecting a relatively thick anteroposterior ulna, it is likely that this index may have also been influenced by the short curved ulna. Overall, the forelimb of *H. glaber* show smaller areas for the insertion of pectoral and deltoid muscles, and reduced robustness suggesting a comparatively less efficient scratch-digging ability. Regarding the hindlimb, *H. glaber* showed the smaller tibial spine (low TSI) among bathyergids (Figure 4). This feature, along with the lack of distal tibio-fibular ossification, and thinner femur (also in *F. damarensis*) reflected a reduced robustness of the hindlimb.

Altogether, these features indicate a considerably reduced fossorial ability for the limbs of *H. glaber*, probably affecting multiple functions during burrowing, such as the efficiency of parasagittal scratch-digging, stabilization and shock absorption of the shoulder, resistance for bending and torsional loads imposed by muscles, and retraction/flexion of muscles and strength of the knee (e.g., Carleton, 1941; Samuels and Van Valkenburgh, 2008; Steiner-Souza et al., 2010). Such reduced fossorial ability is in concordance with the reduced claws of this species among bathyergids (Figure 1), suggesting a considerable relegated function of limbs to break up soils (see also Samuels and Van Valkenburgh, 2008). Instead, such features indicate a more gracile appendicular morphology in this species and a wider range of motion and flexibility of limbs, which may be beneficial to prioritize bidirectional locomotion and turning around within narrow spaces, particularly when colonies can reach a high number of individuals, e.g., up to 300 individuals (Jarvis et al., 1994). Nevertheless, like other bathyergids, *H. glaber* also exhibits well-developed fossorial traits in their limbs, including a well-developed olecranon process (high IFA) and well-developed third trochanter (Montoya-Sanhueza et al., 2022a), the former being even more developed than in *B. suillus* (Figure 3). The long bones of *H. glaber* are also composed of thick cortical walls and experience scarce bone resorption during ontogeny (Pinto et al., 2010; Montoya-Sanhueza et al., 2021a,b), like other bathyergids (Montoya-Sanhueza and Chinsamy, 2017; Montoya-Sanhueza, 2020), allowing them to be more resistant to high impact activities. These latter features may represent important attributes to compensate for the lack of specialization in other regions of the appendicular skeleton.

The reduced robustness in the long bones of *H. glaber* rather resembles that of non-fossorial mammals including their closest outgroup relatives, *Petromys typicus* (Petromuridae), *Thryonomys swinderianus* (Thryonomyidae), and *Hystrix africae australis* (Hystricidae) (Montoya-Sanhueza et al., 2022a). The proximal section of the humerus is also similar to that of terrestrial mammals with a more generalized bone morphology such as the tenrecid *Setifer* and *Tenrec*, while the distal humerus is more similar to that of the erinaceid, *Echinosorex* (Salton and Sargis, 2008). The unfused tibia-fibula of *H. glaber* is more similar to the generalized condition found in hystricognaths (De Graaff, 1979), including *P. typicus* (a rock climber), *T. swinderianus* (semi-aquatic/semi-fossorial), and *H. africae australis* (ambulatorial/semi-fossorial), thus providing further evidence for the basal position of *H. glaber* within the family (Montoya-Sanhueza et al., 2022a, and references therein). Such closely related taxa also have very reduced third trochanters and less specialized olecranon process, although a well-defined deltoid tuberosity (Montoya-Sanhueza et al., 2022a). The lack of a projected deltoid tuberosity in *H. glaber*, and its presence in *P. typicus*, *T. swinderianus*, and *H. africae australis* suggest a considerable reduction during the evolution of *Heterocephalus*, probably occurring in the ancestors or early extinct members of the family. This was proved correct after the analysis of the extinct *Bathyergoides neotertiarius* from the early Miocene of East Africa and Namibia, one of the proposed ancestors of bathyergids (Lavocat, 1973; Bento Da Costa and Senut, 2022). This taxon is more similar to *H. glaber* than to the more recent bathyergids, showing a considerably reduced deltoid tuberosity (although more developed than in *H. glaber*), lack of distal tibio-fibular fusion, a long tail, and a less robust femur with a highly reduced third trochanter (Lavocat, 1973; Bento Da Costa and Senut, 2022). Based on these set of features, it was proposed that *Ba. neotertiarius* had a comparatively reduced fossorial ability (Lavocat, 1973; Bento Da Costa and Senut, 2022), suggesting that early bathyergids may have had a comparatively more restricted use of the subterranean ecotope, and that the evolution of the appendicular fossorial phenotype in Bathyergoidea (Bathyergoididae + Bathyergidae) occurred gradually, and was only fully acquired after the split of *H. glaber* from the rest of the other bathyergids (Montoya-Sanhueza et al., 2022a).

Importantly, the morphological disparity observed in *H. glaber* is unlikely to be the result of prolonged life in captivity. Although life in captivity can have strong effects on the skeleton, particularly associated with disorders of the mineral metabolism and skeletal disuse (O'Regan and Kitchener, 2005), early studies of wild individuals of *H. glaber* have reported a similar phenotype as our captivity sample, e.g., individuality of tibia and fibula, variable shape of the humeral head (flattened and a less pronounced humeral neck), relatively thin distal

humerus, very thin anteroposterior humeral diaphysis, and curved ulna (Parona and Cattaneo, 1893; Hamilton, 1928; Hill et al., 1957). In this respect, previous studies mentioned the fused condition of the distal tibial and fibular epiphyses in bathyergids (De Graaff, 1979; Patterson and Upham, 2014, and references therein), although they did not recognize the particular morphology of *H. glaber* among the family. Muscle activity plays a major role in the stimulation of normal size, shape and architecture of bones, so that muscle force and bone morphology have a reciprocal relationship (Burger and Veldhuijzen, 1993; Whedon and Heaney, 1993; Hillam and Skerry, 1995). Muscle dysfunctions result in alteration of bone composition and geometry, even at prenatal stages (e.g., Sharir et al., 2011). For this reason, it would be expected that living in captivity would affect the normal bone growth of the individuals studied here, especially considering the prolonged time that these colonies have been inbred (more than 20 years), and the fact the such colonies lacked real substrates to dig. However, these colonies show a wide repertoire of digging behaviors. We provide video recordings of active digging (Supplementary Video 1) in different members of the naked mole-rat colony housed at the University of Cape Town (Cape Town, South Africa), which demonstrates that members of the colony are able to perform both chisel-tooth digging and scratch-digging, as well as potent synchronized kicks with the hindlimbs, where the animal uses backward locomotion to simulate the expulsion of soils out of the burrow. It is likely that the constant digging in these colonies have had a positive impact on stimulating normal muscle function, and therefore bone growth and morphology. This represents one of the clearest lines of evidence supporting the idea that the phenotype of *H. glaber* has not been considerably affected by being held in captivity, at least by disuse conditions. Other studies using captive individuals from other colonies have also reported normal bone development, at least for femora, vertebrae and cranium (e.g., Dengler-Crish and Catania, 2007; Pinto et al., 2010; Carmeli-Ligati et al., 2019). Overall, the limb phenotype of naked mole-rats from captive colonies is assumed to not vary considerably from that of wild specimens, although we do not discard the possibility that natural digging regimes in the wild, involving different load magnitudes and frequencies of muscular activity, may also have an impact on other aspects of bone structure such as its bone geometry. Further examinations of wild specimens are needed to assess such hypothesis.

Conclusion

The appendicular anatomy of bathyergids shows clear specializations associated with fossoriality. However, our data demonstrates that scratch-digging bathyergids may not require the highest levels of limb bone specialization, and that both solitary and social chisel-tooth diggers can exhibit

equally or more specialized humero-ulnar joints and tibio-fibular features. Differences in habitat characteristics and soil parameters occupied by mole-rats may help explain such differences, suggesting that cranial specializations are not the unique relevant aspect of digging performance, and that the limb anatomy of chisel-tooth diggers represents an important burrowing tool to maximize the entire process of burrow construction. Such organismal combination of cranial and postcranial adaptations may have played an important role on the dispersion and colonization of African mole-rats to a diverse range of habitats in sub-Saharan Africa (and in turn restricted the distribution of some morphologically divergent taxa such as *B. suillus* and *H. glaber*). Despite the enigmatic disparity of *H. glaber* with the rest of the social bathyergids, it is probable that a combination of historical and ecological characteristics in *H. glaber* involving heterochrony, hyperspecialized cranial apparatus, formation of organized digging sequences and large colony sizes, have all contributed to reduce the selective advantage of a highly specialized appendicular anatomy (see Montoya-Sanhueza et al., 2022a). Our results also showed that most interspecific differences were associated with the zeugopodial elements, suggesting that limb specialization is more prone to occur in the lower parts of the appendicular system, and that the stylopods may represent more conservative elements, probably associated with the multifunctional nature of the humerus and femur. The analysis of a large sample of individuals allowed us to uncover the high degree of morphological variation and developmental plasticity within *H. glaber* (see also Montoya-Sanhueza et al., 2022a, 2021b), whereby further studies on these animals should consider the inclusion of representative samples of the population, as well as the inclusion of wild specimens. Additional studies on burrowing behavior and habitat characterization of African mole-rats would greatly contribute to our understanding of the morphological evolution of this group.

Data availability statement

The original contributions presented in this study are included in the article/Supplementary material, further inquiries can be directed to the corresponding author.

Ethics statement

Ethical review and approval was not required for the animal study because our material is composed of skeletons from old specimens collected many years ago, and/or from previous studies.

Author contributions

GM-S and AC designed the study. NB and RŠ provided mole-rat specimens and supported the experimental procedures. GM-S analyzed the data, prepared the manuscript, acquired images, and created the figures. All authors read, edited, and approved the manuscript.

Funding

This project was supported by the Becas Chile, Government of Chile (CONICYT, 72160463), the National Research Foundation (NRF-117716), the SARChI Chair of Mammalian Behavioral Ecology and Physiology (GUN 64756), and Czech Science Foundation Project GAČR (20-10222S).

Acknowledgments

We thank Emeritus Associate Prof. Jenny Jarvis (University of Cape Town) for providing mole-rat specimens and allowing the recording of the naked mole-rat colonies. Without her support this study would have not been possible. We are very grateful of Prof. Marcelo Sánchez-Villagra (Universität Zürich) for his support during the completion of this study. We thank Prof. Tim Clutton-Brock for providing mole-rat specimens and his team for assisting with the access to specimens in the Kalahari Meerkat Project (Kuruman Station). We also thank

References

- Álvarez, G. I., Díaz, A. O., Longo, M. V., Becerra, F., and Vassallo, A. I. (2012). Histochemical and morphometric analyses of the musculature of the forelimb of the subterranean rodent *Ctenomys talarum* (Octodontidae). *Anat. Histol. Embryol.* 41, 317–325. doi: 10.1111/j.1439-0264.2012.01137.x
- Barčiová, L., Šumbera, R., and Burda, H. (2009). Variation in the digging apparatus of the subterranean silvery mole-rat, *Heliophobius argenteocinereus* (Rodentia, Bathyergidae): The role of ecology and geography. *Biol. J. Linn. Soc.* 97, 822–831.
- Bennett, N. C., and Faulkes, C. G. (2000). *African Mole Rats: Ecology and Eusociality*. Cambridge, UK: Cambridge University Press.
- Bennett, N. C., and Jarvis, J. U. M. (2004). *Cryptomys damarensis*. *Mamm. Species* 756, 1–5.
- Bennett, N. C., Faulkes, C. G., Hart, L., and Jarvis, J. (2009). *Bathyergus suillus* (Rodentia: Bathyergidae). *Mamm. Species* 828, 1–7.
- Bennett, N. C., Jarvis, J. U. M., and Davies, K. C. (1988). Daily and seasonal temperatures in the burrows of African rodent moles. *South Afr. J. Zool.* 23, 189–195.
- Bennett, N. C., Jarvis, J. U. M., and Wallace, D. B. (1990). The relative age structure and body masses of complete wild-captured colonies of two social mole-rats, the common mole-rat, *Cryptomys hottentotus hottentotus* and the Damaraland mole-rat, *Cryptomys damarensis*. *J. Zool.* 220, 469–485.
- Bento Da Costa, L., and Senut, B. (2022). Skeleton of early miocene *Bathyergoides neotertiarius* Stromer, 1923 (Rodentia, Mammalia) from Namibia: Behavioural implications. *Geodiversitas* 44, 291–322.
- Berkovitz, B., and Faulkes, C. G. (2001). Eruption rates of the mandibular incisors of naked mole-rats (*Heterocephalus glaber*). *J. Zool.* 255, 461–466.
- Berkovitz, B., and Shellis, P. (2018). “Lagomorpha and Rodentia (Chapter 7),” in *The Teeth of Mammalian Vertebrates*, eds B. Berkovitz and P. Shellis (Cambridge: Academic Press), 105–143.
- Böhmer, C., Theil, J.-C., Fabre, A.-C., and Herrel, A. (2020). *Atlas of Terrestrial Mammal Limbs (1st ed.)*. Boca Raton, FL: CRC Press.
- Burda, H., Honeycutt, R., and Begall, S. (2002). Are naked and common mole-rats eusocial and if so, why? *Behav. Ecol. Sociobiol.* 47, 293–303.
- Burger, E. H., and Veldhuijzen, J. P. (1993). “Influence of mechanical factor on bone formation, resorption and growth in vitro,” in *Bone Volumen 7 Bone Growth - B*, ed. B. K. Hall (Boca Raton, FL: CRC Press), 368.
- Carleton, A. (1941). A comparative study of the inferior tibio-fibular joint. *J. Anat. Lond.* 76, 45–55.
- Carmeli-Ligati, S., Shipova, A., Dumont, M., Holtze, S., Hildebrandt, T., and Shahar, R. (2019). The structure, composition and mechanical properties of the skeleton of the naked mole-rat (*Heterocephalus glaber*). *Bone* 128:115035. doi: 10.1016/j.bone.2019.115035
- Caspar, K. R., Müller, J., and Begall, S. (2021). Effects of sex and breeding status on skull morphology in cooperatively breeding ansell’s mole-rats and an appraisal of sexual dimorphism in the bathyergidae. *Front. Ecol. Evol.* 9:638754. doi: 10.3389/fevo.2021.638754
- Collis-George, N. (1959). The physical environment of soil animals. *Ecology* 40, 550–557.

Sabine Begall (Universität Duisburg-Essen) for her constructive comments on the study. Two reviewers are acknowledged for their constructive comments on the manuscript, which significantly improved our study.

Conflict of interest

The authors declare that the research was conducted in the absence of any commercial or financial relationships that could be construed as a potential conflict of interest.

Publisher’s note

All claims expressed in this article are solely those of the authors and do not necessarily represent those of their affiliated organizations, or those of the publisher, the editors and the reviewers. Any product that may be evaluated in this article, or claim that may be made by its manufacturer, is not guaranteed or endorsed by the publisher.

Supplementary material

The Supplementary Material for this article can be found online at: <https://www.frontiersin.org/articles/10.3389/fevo.2022.857474/full#supplementary-material>

- Cuthbert, K. (1975). *Burrowing And The Associated Modifications In The Mole-Rats *Bathyergus Suillus* And *Georchus Capensis* - A Comparative Study*. Cape Town: Zoology Honours Project, University of Cape Town.
- Davies, K. C., and Jarvis, J. U. M. (1986). The burrow systems and burrowing dynamics of the mole-rats *Bathyergus suillus* and *Cryptomys hottentotus* in the fynbos of the south-western Cape, South Africa. *J. Zool.* 209, 125–147.
- De Graaff, G. (1979). Molerats (Bathyergidae, Rodentia) in South African National Parks: Notes on the Taxonomic "isolation" and Hystricomorph Affinities of the family. *Koedoe* 22:a653.
- Dengler-Crish, C. M., and Catania, K. C. (2007). Phenotypic plasticity in female naked mole-rats after removal from reproductive suppression. *J. Exp. Biol.* 210, 4351–4358.
- Doubell, N. S., Sahd, L., and Kotzé, S. H. (2020). Comparative forelimb morphology of scratch-digging and chisel-tooth digging African mole-rat species. *J. Morphol.* 281, 1029–1046. doi: 10.1002/jmor.21229
- Echeverría, A. I., Becerra, F., and Vassallo, A. (2014). Postnatal ontogeny of limb proportions and functional indices in the subterranean rodent *Ctenomys talarum* (Rodentia: Ctenomyidae). *J. Morphol.* 275, 902–913. doi: 10.1002/jmor.20267
- Eilam, D., Adjijes, M., and Vilensky, J. (1995). Uphill locomotion in mole rats: A possible advantage of backward locomotion. *Physiol. Behav.* 58, 483–489. doi: 10.1016/0031-9384(95)00076-u
- Elissamburu, A., and Vizcaíno, S. F. (2004). Limb proportions and adaptations in caviomorph rodents (Rodentia: Caviomorpha). *J. Zool.* 262, 145–159.
- Ellerman, J. R. (1956). The subterranean mammals of the world. *Trans. R. Soc. S. Afr.* 35, 11–20.
- Fournier, M., Hautier, L., and Gomes Rodrigues, H. (2021). Evolution towards fossoriality and morphological convergence in the skull of spalacidae and bathyergidae (Rodentia). *J. Mamm. Evol.* 28, 979–993.
- Gambaryan, P. P., and Gasc, J.-P. (1993). Adaptive properties of the musculoskeletal system in the mole-rat *Myospalax myospalax* (Mammalia, Rodentia), cinefluorographical, anatomical and biomechanical analyses of the burrowing. *Zool. Jahrbuch Anat.* 123, 363–401.
- Gomes Rodrigues, H., and Šumbera, R. (2015). Dental peculiarities in the silvery mole-rat: An original model for studying the evolutionary and biological origins of continuous dental generation in mammals. *PeerJ* 3:e1233. doi: 10.7717/peerj.1233
- Gomes Rodrigues, H., Marangoni, P., Šumbera, R., Tafforeau, P., Wendelen, W., and Viriot, L. (2011). Continuous dental replacement in a hyper-chisel tooth digging rodent. *Proc. Natl. Acad. Sci. U.S.A.* 108, 17355–17359. doi: 10.1073/pnas.1109615108
- Gomes Rodrigues, H., Šumbera, R., and Hautier, L. (2016). Life in burrows channelled the morphological evolution of the skull in rodents: The case of African mole-rats (Bathyergidae, Rodentia). *J. Mamm. Evol.* 23, 175–189. doi: 10.1007/s10914-015-9305-x
- Greene, E. C. (1935). The anatomy of the rat. *Trans. Am. Philos. Soc.* 27, 1–370.
- Hamilton, W. J. Jr. (1928). *Heterocephalus*, the remarkable African burrowing rodent. *Mus. Brooklyn Inst. Arts Sci.* 3, 173–191.
- Hammer, Ø, Harper, D. A. T., and Ryan, P. D. (2001). PAST: Paleontological statistics software package for education and data analysis. *Palaentol. Electron.* 4, 1–9.
- Hart, L., Chimimba, C. T., Jarvis, J. U. M., O'Riain, J., and Bennett, N. C. (2007). Craniometric sexual dimorphism and age variation in the South African Cape Dune Mole-Rat (*Bathyergus suillus*). *J. Mammal.* 88, 657–666.
- Hildebrand, M. (1978). Insertions and functions of certain flexor muscles in the hind leg of rodents. *J. Morphol.* 155, 111–122. doi: 10.1002/jmor.1051550108
- Hildebrand, M. (1985). "Digging of quadrupeds," in *Functional Vertebrate Morphology*, eds M. Hildebrand, D. Bramble, K. Liem, and D. B. Wake (Massachusetts: The Belknap Press of Harvard University Press), 89–109.
- Hill, W. C., Porter, A., Bloom, T. J., Seago, A., and Southwick, D. (1957). Field and laboratory studies on the naked mole-rat (*Heterocephalus glaber*). *Proc. Zool. Soc. Lond.* 128, 455–513.
- Hillam, R., and Skerry, T. M. (1995). Inhibition of bone resorption and stimulation of formation by mechanical loading of the modeling rat ulna *In Vivo*. *J. Bone Miner. Res.* 10, 683–689. doi: 10.1002/jbmr.5650100503
- Holliger, C. D. (1916). Anatomical adaptations in the thoracic limb of the California pocket gopher and other rodents. *Zool. Univ. Calif. Publ.* 13, 447–494.
- Houslay, T. M., Vulliou, P., Zöttl, M., and Clutton-Brock, T. H. (2020). Benefits of cooperation in captive Damaraland mole-rats. *Behav. Ecol.* 31, 711–718.
- Howell, B. (1965). *Speed In Mammals, Their Specialization For Running And Leaping*. New York, NY: Hafner Publishing Company.
- IBM Corp (2017). *IBM SPSS Statistics for Windows, Version 25.0*. Armonk, NY: IBM Corp.
- Jarvis, J. U. M., and Bennett, N. C. (1993). Eusociality has evolved independently in two genera of bathyergid mole-rats – but occurs in no other subterranean mammal. *Behav. Ecol. Sociobiol.* 33, 253–260.
- Jarvis, J. U. M., and Sale, J. (1971). Burrowing and burrow patterns of East African mole-rats *Tachyoryctes*, *Heliophobius* and *Heterocephalus*. *J. Zool.* 163, 451–479.
- Jarvis, J. U. M., and Sherman, P. W. (2002). *Heterocephalus glaber*. *Mamm. Species* 706, 1–9.
- Jarvis, J. U. M., Bennett, N. C., and Spinks, A. C. (1998). Food availability and foraging by wild colonies of Damaraland mole-rats (*Cryptomys damarensis*): Implications for sociality. *Oecologia* 113, 290–298. doi: 10.1007/s004420050380
- Jarvis, J. U. M., O'Riain, M. J., Bennett, N. C., and Sherman, P. W. (1994). Mammalian eusociality: A family affair. *Trends Ecol. Evol.* 9, 47–51. doi: 10.1016/0169-5347(94)90267-4
- Klein, R. G. (1991). Size variation in the Cape dune mole-rat (*Bathyergus suillus*) and late Quaternary climatic change in the southwestern Cape Province, South Africa. *Quat. Res.* 36, 243–256.
- Kraus, A. M. B., Lövy, M., Mikula, O., Okrouhlik, N. C., Bennett, A., Herrel, et al. (2022). Bite force in strictly subterranean rodent family, African mole-rats (*Bathyergidae*): The role of digging mode, social organisation, and ecology. *Funct. Ecol.* 36:162. doi: 10.1111/1365-2435.14132
- Kubiak, B., Maestri, R., de Almeida, T. S., Borges, L. R., Galiano, D., Fornel, R., et al. (2018). Evolution in action: Soil hardness influences morphology in a subterranean rodent (Rodentia: Ctenomyidae). *Biol. J. Linn. Soc.* 125, 766–776.
- Lavocat, R. (1973). *Les Rongeurs du Miocène d'Afrique Orientale. 1. 1, Miocène inférieur, Texte*. Montpellier: Ecole pratique des hautes études, 1–284.
- Le Comber, S. C., Spinks, A. C., Bennett, N. C., Jarvis, J. U. M., and Faulkes, C. G. (2002). Fractal dimension of African mole-rat burrows. *Can. J. Zool.* 80, 436–441.
- Lehmann, W. H. (1963). The forelimb architecture of some fossorial rodents. *J. Morphol.* 113, 59–76.
- Lilje, K. E., Tardieu, C., and Fischer, M. S. (2003). Scaling of long bones in ruminants with respect to the scapula. *J. Zool. Syst. Evol. Res.* 41, 118–126.
- Lin, Y.-F., Chappuis, A., Rice, S., and Dumont, E. R. (2017). The effects of soil compactness on the burrowing performance of sympatric eastern and hairy-tailed moles. *J. Zool.* 301, 310–319.
- Lövy, M., Škliba, J., Burda, H., Chitaukali, W. N., and Šumbera, R. (2012). Ecological characteristics in habitats of two African mole-rat species with different social systems in an area of sympatry: Implications for the mole-rat social evolution. *J. Zool.* 286, 145–153.
- Luna, F., and Antinuchi, C. D. (2006). Cost of foraging in the subterranean rodent *Ctenomys talarum*: Effect of soil hardness. *Can. J. Zool.* 84, 661–667.
- Luna, F., Antinuchi, C. D., and Busch, C. (2002). Digging energetics in the South American rodent, *Ctenomys talarum* (Rodentia, Ctenomyidae). *Can. J. Zool.* 80, 2144–2149.
- Marcy, A. E., Fendorf, S., Patton, J. L., and Hadly, E. A. (2013). Morphological Adaptations for Digging and Climate-Impacted Soil Properties Define Pocket Gopher (*Thomomys* spp.) Distributions. *PLoS One* 8:e64935. doi: 10.1371/journal.pone.0064935
- Mason, M. J., Cornwall, H. L., and Smith, E. S. J. (2016). Ear structures of the naked mole-rat, *Heterocephalus glaber*, and its relatives (Rodentia: Bathyergidae). *PLoS One* 11:e0167079. doi: 10.1371/journal.pone.0167079
- McIntosh, A. F., and Cox, P. G. (2016a). The impact of gape on the performance of the skull in chisel-tooth digging and scratch digging mole-rats (Rodentia: Bathyergidae). *R. Soc. Open Sci.* 3:160568. doi: 10.1098/rsos.160568
- McIntosh, A. F., and Cox, P. G. (2016b). Functional implications of craniomandibular morphology in African mole -rats (Rodentia: Bathyergidae). *Biol. J. Linn. Soc.* 117, 447–462.
- Montoya-Sanhueza, G. (2020). *Functional Anatomy, Osteogenesis and Bone Microstructure of the Appendicular System of African Mole-Rats (Rodentia: Ctenomyidae: Bathyergidae)*. Ph D. thesis. Cape Town: University of Cape Town.
- Montoya-Sanhueza, G., and Chinsamy, A. (2017). Long bone histology of the subterranean rodent *Bathyergus suillus* (Bathyergidae): Ontogenetic pattern of cortical bone thickening. *J. Anat.* 230, 203–233. doi: 10.1111/joa.12547
- Montoya-Sanhueza, G., and Chinsamy, A. (2018). Cortical bone adaptation and mineral mobilization in the subterranean mammal *Bathyergus suillus* (Rodentia: Bathyergidae): Effects of age and sex. *PeerJ* 6:e4944. doi: 10.7717/peerj.4944
- Montoya-Sanhueza, G., Bennett, N. C., Oosthuizen, M. K., Dengler-Crish, C. M., and Chinsamy, A. (2021a). Long bone histomorphogenesis of the naked mole-rat: Histodiversity and intraspecific variation. *J. Anat.* 238, 1259–1283. doi: 10.1111/joa.13381

- Montoya-Sanhueza, G., Bennett, N. C., Oosthuizen, M. K., Dengler-Criss, C. M., and Chinsamy, A. (2021b). Bone remodeling in the longest living rodent, the naked mole-rat: Interelement variation and the effects of reproduction. *J. Anat.* 239, 81–100. doi: 10.1111/joa.13404
- Montoya-Sanhueza, G., Šaffa, G., Šumbera, R., Chinsamy, A., Jarvis, J. U. M., and Bennett, N. C. (2022a). Fossorial adaptations in African mole-rats (Bathyergidae) and the unique appendicular phenotype of naked mole-rats. *Commun. Biol.* 5:526. doi: 10.1038/s42003-022-03480-z
- Montoya-Sanhueza, G., Šumbera, R., Bennett, N. C., and Chinsamy, A. (2022b). Developmental Plasticity in the Ossification of the Proximal Femur of *Heterocephalus glaber* (Bathyergidae, Rodentia). *J. Mammal. Evol.* 29, 663–675. doi: 10.1007/s10914-022-09602-y
- Montoya-Sanhueza, G., Wilson, L. A. B., and Chinsamy, A. (2019). Postnatal development of the largest subterranean mammal (*Bathyergus suillus*): Morphology, osteogenesis, and modularity of the appendicular skeleton. *Dev. Dyn.* 248, 1101–1128. doi: 10.1002/dvdy.81
- Moore Crisp, A., Barnes, C. J., and Lee, D. V. (2019). Tunnel-tube and Fourier methods for measuring three-dimensional medium reaction force in burrowing animals. *J. Exp. Biol.* 222:jeb213553. doi: 10.1242/jeb.213553
- Moss, M. L. (1977). A functional analysis of fusion of the tibia and fibula in the rat and mouse. *Acta Anat.* 97, 321–332. doi: 10.1159/000144749
- O'Regan, H. J., and Kitchener, A. C. (2005). The effects of captivity on the morphology of captive, domesticated and feral mammals. *Mamm. Rev.* 35, 215–230.
- Oosthuizen, M. K., and Bennett, N. C. (2022). Clocks Ticking in the Dark: A Review of Biological Rhythms in Subterranean African Mole-Rats. *Front. Ecol. Evol.* 10:878533. doi: 10.3389/fevo.2022.878533
- Parona, C., and Cattaneo, G. (1893). Note anatomiche e zoologiche sull' *Heterocephalus*, Ruppel. *Ann. Mus. Civ. Storia Nat. Genova* 13, 419–446.
- Patterson, B. D., and Upham, N. S. (2014). A newly recognized family from the Horn of Africa, the Heterocephalidae (Rodentia: Ctenohipstrica). *Zool. J. Linn. Soc.* 172, 942–963.
- Pinto, M., Jepsen, K. J., and Terranova, C. J. (2010). Lack of sexual dimorphism in femora of the eusocial and hypogonadic naked mole-rat: A novel animal model for the study of delayed puberty on the skeletal system. *Bone* 46, 112–120. doi: 10.1016/j.bone.2009.08.060
- Prochel, J., Begall, S., and Burda, H. (2014). Morphology of the carpal region in some rodents with special emphasis on hystricognaths. *Acta Zool.* 95, 220–238.
- Quinn, G., and Keough, M. (2002). *Experimental Design and Data Analysis for Biologists*. Cambridge: Cambridge University Press.
- Rose, M. D. (1989). New postcranial specimens of catarrhines from the Middle Miocene Chinji Formation, Pakistan: Descriptions and a discussion of proximal humeral functional morphology in anthropoids. *J. Hum. Evol.* 18, 131–162.
- Sahd, L., Bennett, N. C., and Kotzé, S. H. (2019). Hind foot drumming: Morphological adaptations of the muscles and bones of the hind limb in three African mole-rat species. *J. Anat.* 235, 811–824.
- Sahd, L., Bennett, N. C., and Kotzé, S. H. (2020). Hind foot drumming: Morphofunctional analysis of the hind limb osteology in three species of African mole-rats (Bathyergidae). *J. Morphol.* 281, 438–449. doi: 10.1002/jmor.21110
- Salton, J. A., and Sargis, E. J. (2008). "Evolutionary Morphology of the Tenrecoidea (Mammalia) Forelimb Skeleton," in *Mammalian Evolutionary Morphology, A Tribute to Frederick S. Szalay*, eds E. Sargis and M. Dagosto (Dordrecht: Springer Netherlands), 51–72.
- Salton, J. A., and Sargis, E. J. (2009). Evolutionary morphology of the Tenrecoidea (Mammalia) hindlimb skeleton. *J. Morphol.* 270, 367–387. doi: 10.1002/jmor.10697
- Samuels, J. X., and Van Valkenburgh, B. (2008). Skeletal Indicators of Locomotor Adaptations in Living and Extinct Rodents. *J. Morphol.* 269, 1387–1411. doi: 10.1002/jmor.10662
- Sharir, A., Stern, T., Rot, C., Shahar, R., and Zelzer, E. (2011). Muscle force regulates bone shaping for optimal load-bearing capacity during embryogenesis. *Development* 138, 3247–3259. doi: 10.1242/dev.063768
- Spinks, A., and Plagányi, É. (1999). Reduced starvation risks and habitat constraints promote cooperation in the common mole-rat, *Cryptomys hottentotus hottentotus*: A computer-simulated foraging model. *Oikos* 85, 435–444.
- Stein, B. (2000). "Morphology of Subterranean Rodents," in *Life Underground: The Biology Of Subterranean Rodents*, eds E. A. Lacey, J. Patton, and G. N. Cameron (Chicago: The University of Chicago Press), 19–61.
- Steiner-Souza, F., De Freitas, T. R. O., and Cordeiro-Estrela, P. (2010). Inferring adaptation within shape diversity of the humerus of subterranean rodent *Ctenomys*. *Biol. J. Linn. Soc.* 100, 353–367.
- Šumbera, R., Mazoch, V., Patzenhauerová, H., Lövy, M., Šklíba, J., Bryja, J., et al. (2012). Burrow architecture, family composition and habitat characteristics of the largest social African mole-rat: The giant mole-rat constructs really giant burrow systems. *Acta Theriol.* 57, 121–130.
- Šumbera, R., Šklíba, J., Elichová, M., Chitaukali, W. N., and Burda, H. (2008). Natural history and burrow system architecture of the silvery mole-rat from *Brachystegia* woodland. *J. Zool.* 274, 77–84.
- Šumbera, R. (2019). Thermal biology of a strictly subterranean mammalian family, the African mole-rats (*Bathyergidae*, *Rodentia*) - a review. *J. Therm. Biol.* 79, 166–189. doi: 10.1016/j.jtherbio.2018.11.003
- Taylor, P., Jarvis, J., Crowe, T., and Davies, K. C. (1985). Age determination in the Cape mole-rat *Georchys capensis*. *S.-Afr. Tydskr. Dierk.* 20, 261–267.
- Thomas, H. G. (2013). *Seasonal Patterns Of Burrow Architecture And Morphological Adaptations To Digging In Three Sympatric Species Of South African Mole-Rat, Bathyergus Suillus (Shreber, 1782), Georchys Capensis (Pallas, 1778) And Cryptomys Hottentotus Hottentotus (Lesson, 1826)*. Ph D. thesis. Pretoria: University of Pretoria.
- Thomas, H. G., Swanepoel, D., and Bennett, N. C. (2016). Burrow architecture of the Damaraland mole-rat (*Fukomys damarensis*) from South Africa. *Afr. Zool.* 51, 29–36.
- Tucker, R. (1981). The digging behavior and skin differentiations in *Heterocephalus glaber*. *J. Morphol.* 168, 51–71. doi: 10.1002/jmor.1051680107
- Uhrová, M., Mikula, O., and Bennett, N. Z. (2022). Species limits and phylogeographic structure in two genera of solitary African mole-rats *Georchys* and *Heliophobius*. *Mol. Phylogenet. Evol.* 167:107337. doi: 10.1016/j.ympev.2021.107337
- Van Daele, P. A., Herrel, A., and Adriaens, D. (2009). Biting performance in teeth-digging African mole-rats (*Fukomys*, *Bathyergidae*, *Rodentia*). *Physiol. Biochem. Zool.* 82, 40–50. doi: 10.1086/594379
- Van Wassenbergh, S., Heindryckx, S., and Adriaens, D. (2017). Kinematics of chisel-tooth digging by African mole-rats. *J. Exp. Biol.* 220, 4479–4485. doi: 10.1242/jeb.164061
- Vassallo, A. I. (1998). Functional morphology, comparative behaviour, and adaptation in two sympatric subterranean rodents genus *Ctenomys* (*Caviomorpha: Octodontidae*). *J. Zool.* 244, 415–427.
- Vassallo, A. I. F., Becerra, A. I., and Echeverría. (2021). "Biomechanics and Strategies of Digging," in *Tuco-Tucos. An Evolutionary Approach to the Diversity of a Neotropical Subterranean Rodent*, eds T. R. O. Freitas, G. L. Gonçalves, and R. Maestri (Berlin: Springer), 141–166.
- Visser, J. H., Bennett, N. C., Jansen, and van Vuuren, B. (2019). Phylogeny and biogeography of the African Bathyergidae: A review of patterns and processes. *PeerJ* 7:e7730. doi: 10.7717/peerj.7730
- Vizcaino, S. F., Bargo, S., Cassini, G. H., and Toledo, N. (2016). *Forma Y Función En Paleobiología De Vertebrados*. La Plata: Editorial de la Universidad de La Plata (EDULP).
- Vizcaino, S. F., Fariña, R. A., and Mazzetta, G. V. (1999). Ulnar dimensions and fossoriality in armadillos. *Acta Theriol.* 44, 309–320.
- Vleck, D. (1979). The energy cost of burrowing by the pocket gopher *Thomomys bottae*. *Physiol. Zool.* 52, 122–136.
- Whedon, D., and Heaney, R. (1993). "Effects of physical inactivity, paralysis, and weightlessness on bone growth," in *Bone Volumen 7 Bone Growth - B*, ed B. K. Hall (Boca Raton, FL: CRC Press), 368.
- Wilson, L. A. B., and Geiger, M. (2015). "Diversity and evolution of femoral variation in Ctenohipstrica," in *Evolution of the Rodents*, eds P. G. Cox and L. Hautier (Cambridge: Cambridge University Press), 510–538.
- Winkler, A. J., Denys, C., and Avery, D. M. (2010). "Cenozoic Mammals of Africa," in *Paleogenetic Analyses Reveal Unsuspected Phylogenetic Affinities between Mice and the Extinct Malpaisomys insularis, an Endemic Rodent of the Canaries*, eds L. Werdelin and W. J. Sanders (Berkeley: University of California Press), 263–305.
- Zelová, J., Šumbera, R., Okrouhlik, J., and Burda, H. (2010). Cost of digging is determined by intrinsic factors rather than by substrate quality in two subterranean rodent species. *Physiol. Behav.* 99, 54–58. doi: 10.1016/j.physbeh.2009.10.007